NASA Contractor Report 168226

GEOMETRICAL ANALYSIS OF CIRCULAR-CUT SPIRAL BEVEL GEARS

Ronald L. Huston

University of Cincinnati
Cincinnati, Ohio

August 1983

Prepared for
NATIONAL AERONAUTICS AND SPACE ADMINISTRATION
Lewis Research Center
Under Grant NSG-3188

TABLE OF CONTENTS

INTRODUCTION

This report summarizes results of recent geometrical studies of circular-cut spiral bevel gear teeth. These studies have been stimulated by interest in determining the effects of slight profile changes on the kinematics, noise, stress analysis, wear, and life of spiral bevel gears. This interest has been stimulated by a desire to improve operating and maintenance procedures in high performance transmissions of helicopters and other aircraft. References [1-6]* are examples of approaches taken to develop a broader understanding of the geometrical characteristics of spiral bevel and hypoid gears. It is believed that a quantitative understanding of the geometrical characteristics is fundamental to analyses of the above mentioned physical phenomena of these gears.

Spiral bevel gears are used in high performance transmissions because their curved teeth provide for a smoother and quieter operation than straight bevel gear teeth. Also, the curved teeth provide greater bending resistance. Figure 1. contains a photo of a spiral bevel gear and its pinion.

These gears are called "spiral" bevel gears since the theoretical centerline of the gear tooth is a logarithmic spiral [7]. A logarithmic spiral has the advantage of providing equal angles between the tooth centerline and radial lines at all points along the centerline. This in turn provides for uniform geometrical characteristics of the tooth profile in the transverse planes of the gears--that is, the planes normal to the radial pitch lines of the gear. However, the disadvantages of logarithmic spiral teeth are that they are difficult to fabricate and the tooth surface itself is often considered to be too "flat" to incorporate the advantages of curved teeth [8]. Therefore, most gear manufacturers have been cutting spiral bevel gears with circular cutters.

---

* Numbers in brackets refer to References at the end of the report.

Indeed, probably more than 90% of the spiral bevel gears currently in use have been made with a circular cutter.

The advantages of circular cutters is that they are relatively easy to use in manufacturing processes and through varying the cutter radius and the position of the cutter center, a variety of toothforms can be produced. Also, for a carefully chosen cutter setting and cutter radius a circular arc can very nearly approximate a logarithmic spiral [7]. A disadvantage of circular cutters is that the uniform tooth profile in the transverse plane is lost, leading to distortions along the centerline.

The analysis presented in this report concentrates on crown gears. A crown gear (sometimes called a "crown rack") is a flat gear and is analogous to a rack for spur gears. Many spiral bevel gears have apex angles which are nearly 90° and they are thus close to being crown gears (See Figure 1.).

Figure 2. depicts a crown gear together with commonly used planes associated with the gear surfaces. The pitch plane is the plane of the gear itself. The axial planes, containing the axis of the gear, are perpendicular to the pitch plane. The transverse planes are perpendicular to both the pitch and axial planes. The transverse planes are thus perpendicular to the radial pitch lines. The normal planes, containing the cutter center, are perpendicular to the pitch plane as shown in Figure 2.

A transverse plane is customarily used in the study of straight tooth bevel gears, while a normal plane is often used in the study of spiral bevel gears [9]. A reason for this difference is that for smooth spiral bevel tooth surfaces the contact forces between mating teeth are transmitted in the normal planes. However, if friction is present the resulting force vector is rotated out of the normal plane and it becomes more nearly parallel to the transverse plane. Therefore, a major portion of the analysis of this report--particularly that dealing with pressure angles--is developed in a transverse plane.

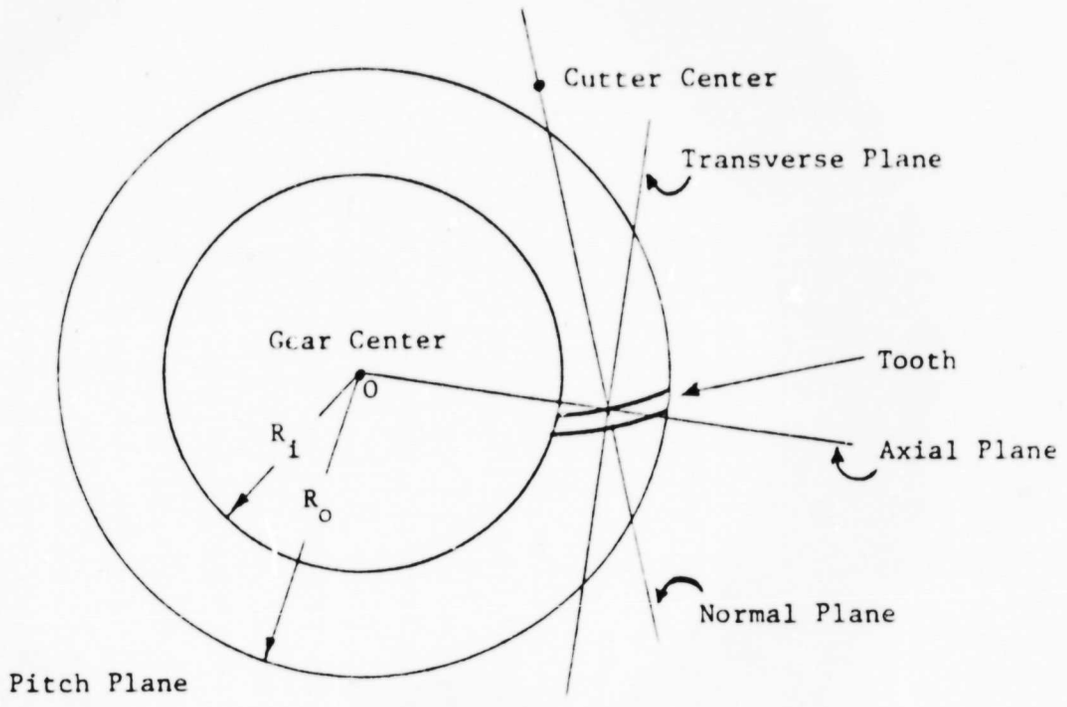

Figure 1. Spiral Bevel Crown Gear and Identifying Planes

Figure 2. A Spiral Bevel Gear and Pinion

The report itself is divided into five parts with the first part providing some preliminary analysis useful in the sequel. The second part discusses tooth profile changes in the transverse planes along the tooth centerline. The cutter profile shape needed to obtain a straight line tooth profile in the transverse plane is developed in the third part. The fourth part of the report presents a procedure for finding the radii of curvature of circular-cut crown gear teeth. The radii of curvature are useful parameters in the study of contact stresses, lubrication, wear, and life of the gears. Specific results are presented for straight, involute, and hyperbolic cutter profiles. A discussion and concluding remarks are presented in the final part.

SYMBOLS

C	Cutter center, curve defining a surface of revolution.
$\underset{\sim}{e}_i (i=1,2)$	Surface base vectors.
g	Determinant of g_{ij}.
$g_{ij} (i,j=1,2)$	Metric tensor coefficients.
$\underset{\sim}{h}_i (i=1,2)$	Fundamental vector defined by Equation (51).
$h_{ij} (i,j=1,2)$	Second fundamental tensor defined by Equation (52).
H,V	Horizontal and vertical cutter settings.
J	Mean curvature
k	Cotangent of pressure angle.
K	Gaussian curvature
$\underset{\sim}{n}$	A unit vector normal to a surface.
$\underset{\sim}{n}_r$	Radial unit vector.
$\underset{\sim}{n}_x, \underset{\sim}{n}_y, \underset{\sim}{n}_z$	Unit vectors parallel to X,Y,Z.
$\underset{\sim}{n}_\theta$	Transverse unit vector.
N	Normal line to a surface of revolution.
O	Gear center.
$\underset{\sim}{P}$	Position vector to a typical point on a curve.
P	Typical point on the gear centerline, or on the gear surface.
P_m	Midpoint on tooth centerline.
r	Radial coordinate from O.
$\hat{r}$	Radial coordinate from C.
R_c	Cutter radius.
R_i	Inner gear radius.
R_m	Mean radial distance.
R_o	Outer gear radius.

R_{max}, R_{min}	Maximum and minimum surface radii of curvature.
S	A general surface.
t_0	Transverse tooth thickness in the pitch plane.
T	Tangent line to C, Tangent point.
u^1, u^2	Surface defining parameters.
x,y,z	Cartesian coordinates relative to the X,Y,Z, coordinate system.
$\hat{x},\hat{y},\hat{z}$	Cartesian coordinates relative to the $\hat{X},\hat{Y},\hat{Z}$ coordinate system.
$\hat{\hat{x}},\hat{\hat{y}},\hat{\hat{z}}$	Cartesian coordinates relative to the $\hat{\hat{X}},\hat{\hat{Y}},\hat{\hat{Z}}$ coordiante system.
X,Y,Z	Coordinate axes with origin at O and with the X-Y plane coincident with the pitch plane.
$\hat{X},\hat{Y},\hat{Z}$	Coordinate axes with origin at C and with the X-Y plane coincident with the pitch plane.
α	Cutter inclination
γ	Angle OPC in Figure 4.
θ	Transverse coordinate, Pressure angle.
κ	Cotangent of the spiral angle.
ξ η	Coordinate axes of Figure 11.
π	Transverse plane.
ρ	Radius of curvature.
ϕ	Transverse angle, Angle between N and the x-axis.
ϕ_m	Mid-transverse angle.
ψ	Spiral angle, Inclination angle.
ψ_m	Mid-spiral angle.

1. Configuration

Figure 3. shows a top view of some of the geometrical features of a circular-cut crown gear, which will be useful in the sequel. Specifically, O is the gear center or "gear apex" and C is the circular cutter center with a cutter radius R_c in the pitch (X-Y) plane. The spiral angle ψ is the angle between a radial line through O and the tooth centerline. The mid-spiral angle ψ_m shown in Figure 2., is the angle between the tooth centerline and the radial line passing through the midpoint of the tooth centerline (the X-axis). Finally, Figure 2. has two sets of coordinate axes X,Y,Z and $\hat{X},\hat{Y},\hat{Z}$ with origins at O and C respectively. The coordinates are then related by the simple expressions:

$$\hat{x} = x - H \ , \quad \hat{y} = y - V \ , \quad \hat{z} = z \tag{1}$$

where H and V are the horizontal and vertical cutter center settings.

2. Spiral Angles

The spiral angle ψ varies along the centerline of the tooth. For example, Figure 4. shows a series of radial lines intersecting the tooth centerline. It is easily seen that the spiral angles are all distinct, that is,

$$\psi_1 \neq \psi_2 \neq \psi_m \neq \psi_3 \neq \psi_4 \tag{2}$$

Figure 4. also shows tranverse lines (edge views of transverse planes) intersecting the tooth centerline and forming "transverse angles" ϕ which are complements of the spiral angles. The transverse angles are also distinct, that is,

$$\phi_1 \neq \phi_2 \neq \phi_m \neq \phi_3 \neq \phi_4 \tag{3}$$

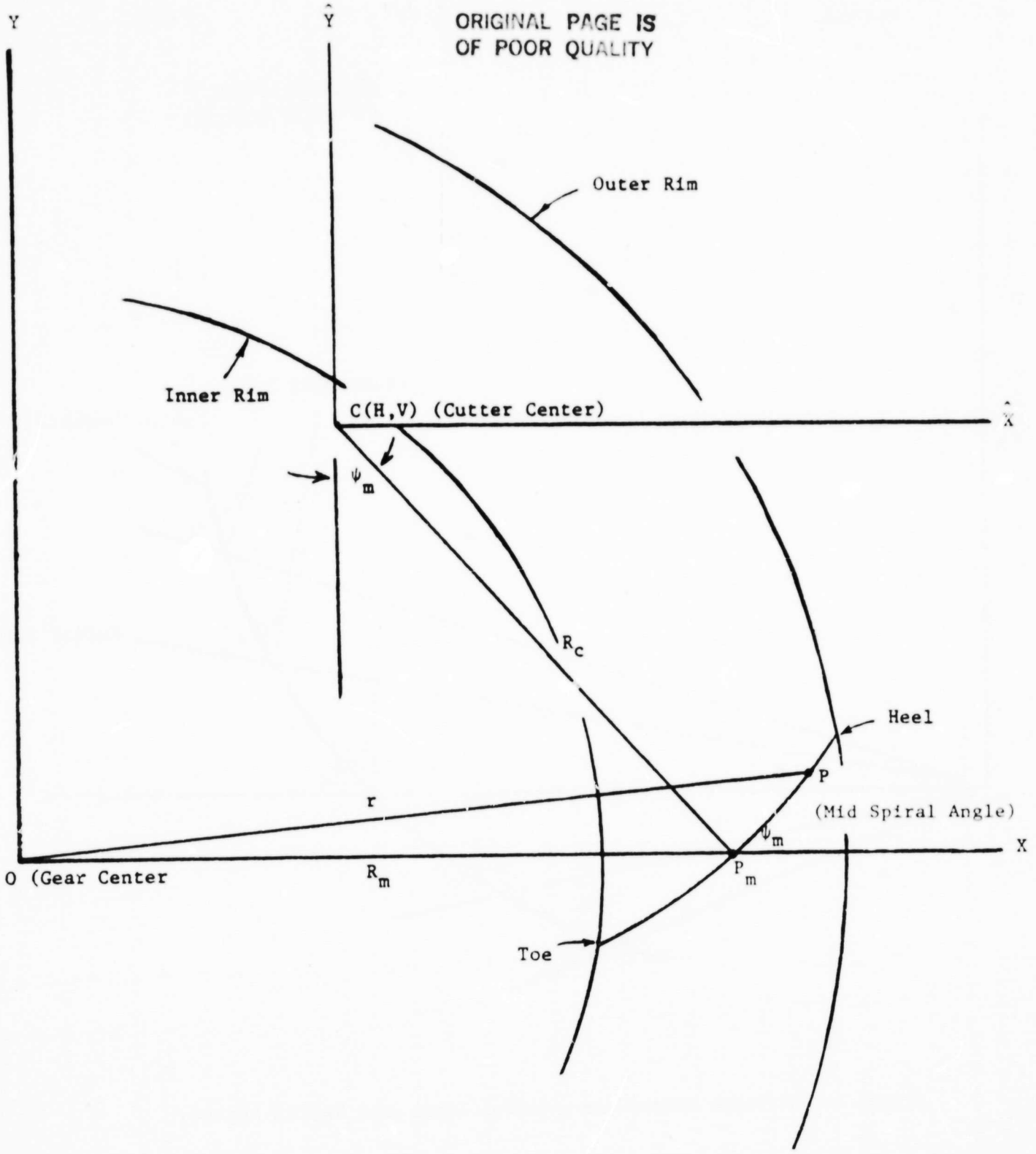

Figure 3. Top View of Circular Cut Crown Gear with the Centerline of a Typical Tooth.

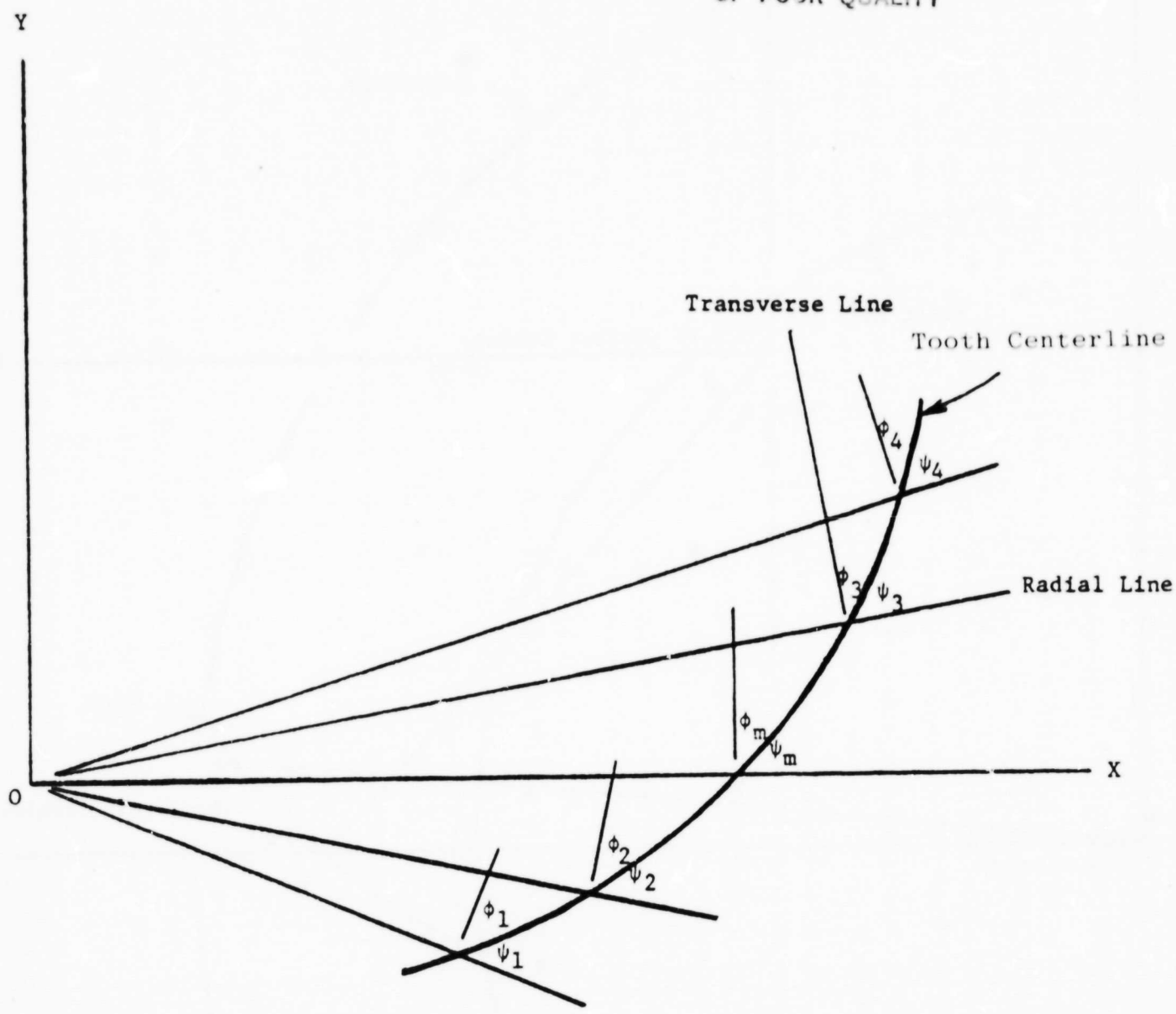

Figure 4 . A Tooth Centerline, Radial Line, and Spiral Angles.

Interestingly, if the tooth centerline is a logarithmic spiral, the spiral angles are all equal. That is,

$$\psi_1 = \psi_2 = \psi_m = \psi_3 = \psi_4 \tag{4}$$

Similarly, the transverse angles are also all equal for a logarithmic spiral tooth centerline. That is,

$$\phi_1 = \phi_2 = \phi_m = \phi_3 = \phi_4 \tag{5}$$

3. Logarithmic Spiral and Circular Arc

The property described by Equations (4) and (3) is an attractive feature of logarithmic spiral tooth centerlines. Indeed, for such a centerline the tooth profiles, obtained by the intersection of the tooth surface and the transverse planes, are all similar.

A logarithmic spiral has an equation of the form

$$r = R_m e^{\kappa\theta} \tag{6}$$

where r and θ are the radial and transverse (polar) coordinates of a typical point P on the curve. For a logarithmic spiral tooth centerline, R_m is the distance from 0 to P_m, the midpoint on the tooth centerline, and κ is the contangent of the spiral angle. That is,

$$\kappa = \cot\psi \tag{7}$$

(Equation (7) follows from Equation (6) by noting that $dr/d\theta = \kappa r$ and that when $\theta = 0$ the slope is: $\tan\psi = \tan\psi_m = rd\theta/dr$.)

Buckingham [7] has shown that there is very little difference between a logarithmic spiral tooth centerline and a circular arc if the radius R_c of the circular arc, is the same as the radius of curvature, at the midpoint P_m, of the logarithmic spiral. It is easily seen (See Section 1. of the APPENDIX) that the radius of curvature of a logarithmic spiral of the form of Equation (6) is:

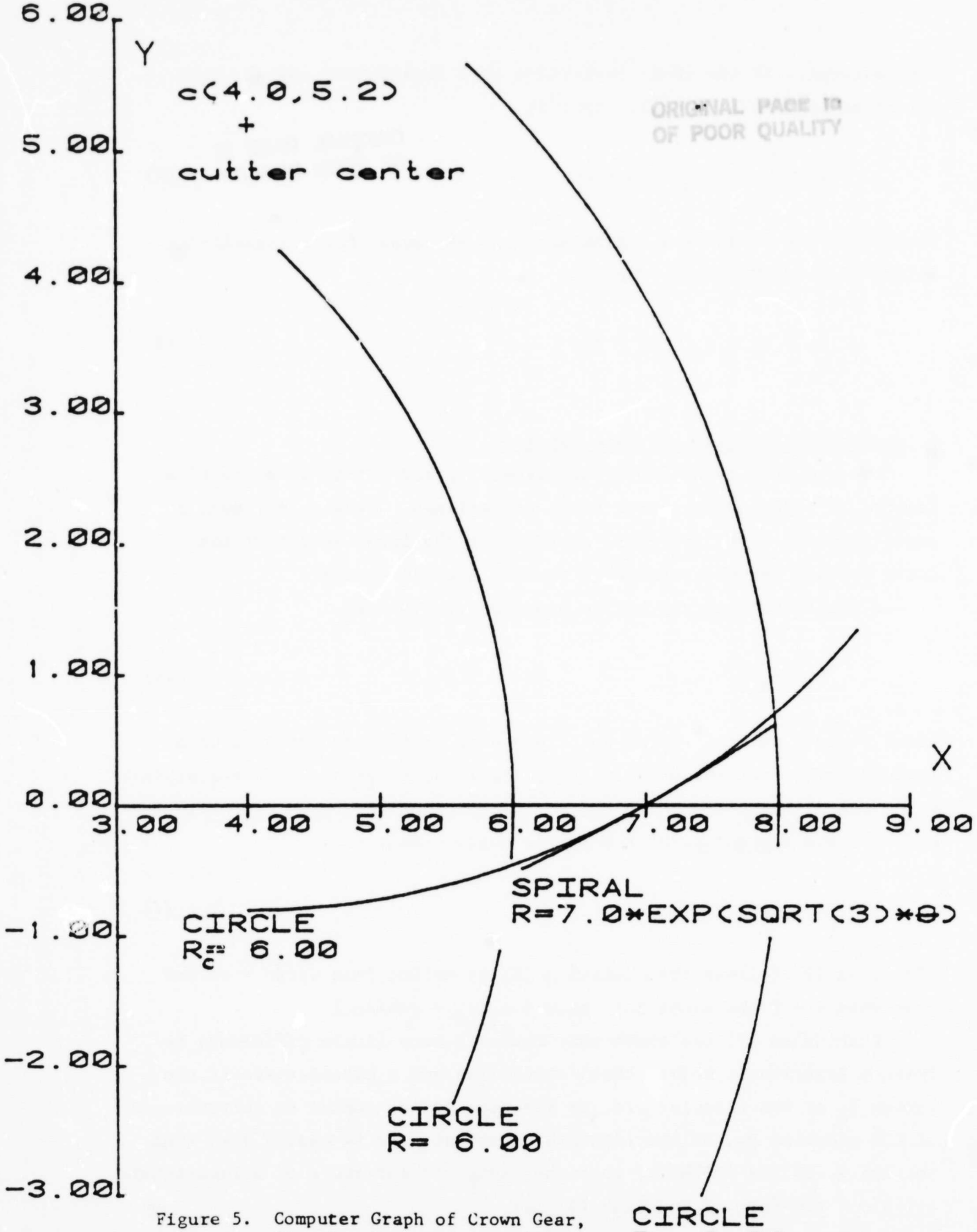

Figure 5. Computer Graph of Crown Gear, Circular Arc, and Logarithmic Spiral.

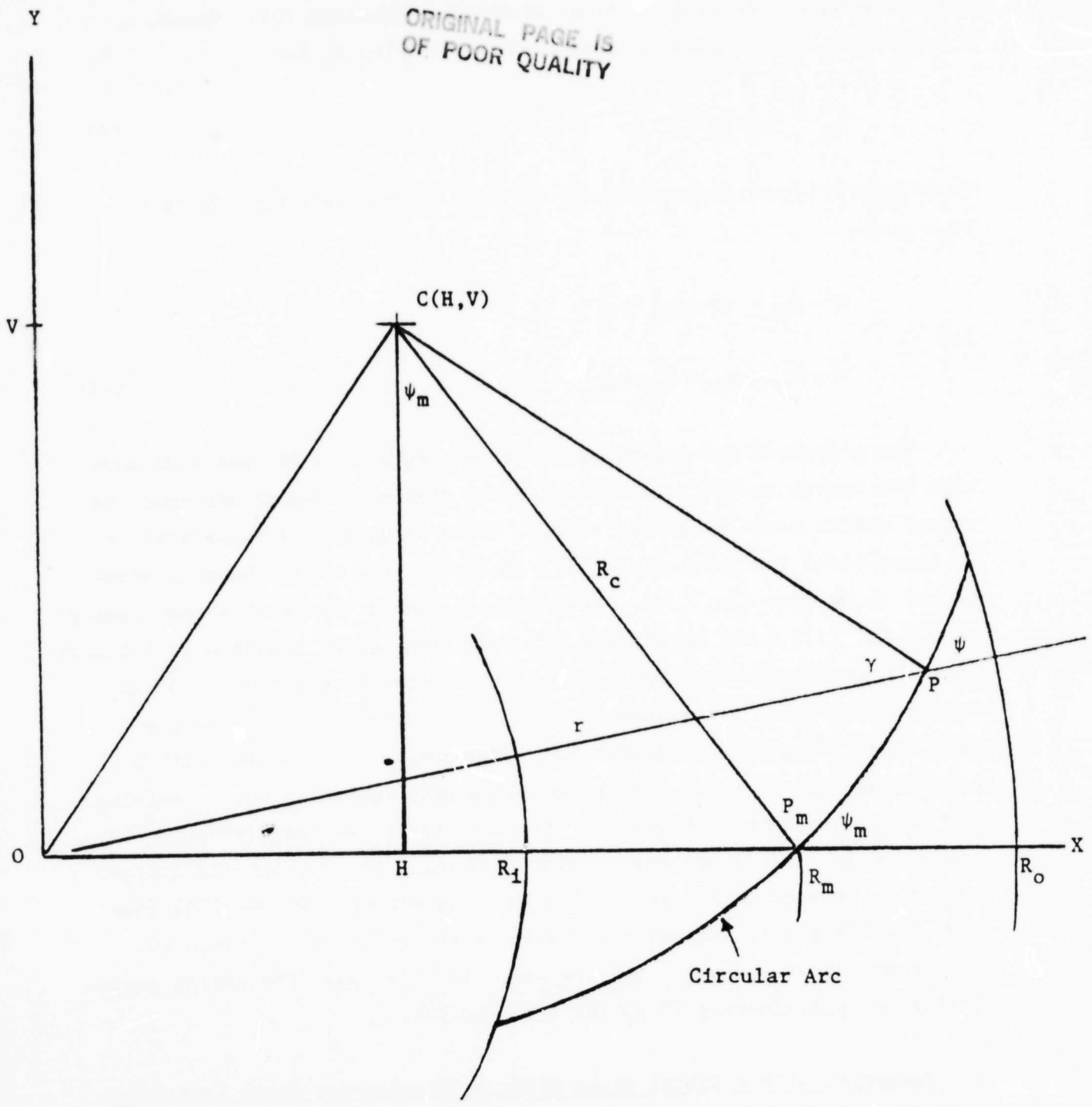

Figure 6. Enlarged View of Circular Arc Tooth Centerline.

$$\rho = r(1 + \kappa)^{\frac{1}{2}} = r/\sin\psi \qquad (8)$$

where the second equality follows from using Equation (7). Hence, a nearly coincident circle is obtained by letting R_c be:

$$R_c = R_m/\sin\psi_m \qquad (9)$$

From Figure 3. the horizontal and vertical cutter settings are then seen to be:

$$H = R_m - R_c\sin\psi_m = 0 \qquad (10)$$

and

$$V = R_c\cos\psi_m = R_m\cot\psi_m \qquad (11)$$

For a typical mid-spiral angle of 30°, Equations (9) and (10) show that the cutter radius would be twice the mean gear radius and that the cutter center would be on the Y-axis. This is sometimes considered to be impractical for fabrication [7]. Moreover, the tooth shape is often deemed to be "too flat" [8]. Nevertheless, for a gear with a mean radius of 7.0 in. (177.8 mm) Buckingham has shown (See also, Equation (14) below) that the difference in spiral angles between the circular arc and the logarithmic spiral centerline at the heel and toe are less than one-half of one degree. A computer plot comparing a circular arc with a logarithmic spiral tooth centerline for a more realistic cutter setting and radius is shown in Figure 5. In this figure the mean radius R_m is again 7.0 in. (177.8 mm) and the midspiral angle is 30°, but the cutter radius is reduced to 6.0 in. (152.4 mm). Equations (10) and (11) then give the horizontal and vertical cutter settings to be: H = 4.0 in. (101.6 mm) and V - $3\sqrt{3}$ in. (132.98 mm). In this case, the spiral angles differ by approximately 6° at the heel and toe.

4. Variation of the Spiral Angle Along a Circular-Cut Tooth Centerline

It is helpful to develop an expression for the change in the spiral angle along a circular arc tooth centerline. Such an expression is easily obtained from Figure 6. which shows an enlarged (but not to scale) view of the circular arc tooth. Then, using the law of cosines with

triangle OPC leads immediately to the expression:

$$(\overline{OC})^2 = (\overline{OP})^2 + (\overline{CP})^2 - 2(\overline{OP})(\overline{CP})\cos\gamma \tag{12}$$

By recognizing that: $\cos\gamma = \sin\psi$, $(\overline{OC})^2 = H^2 + V^2$, $(\overline{OP})^2 = r^2$, and that $(\overline{CP})^2 = R_c^2$, Equation (12) may be rewritten in the form:

$$H^2 + V^2 = r^2 + R_c^2 - 2rR_c\sin\psi$$

or as

$$\sin\psi = (r^2 + R_c^2 - H^2 - V^2)/(2rR_c) \tag{13}$$

Finally, by noting in Figure 6. that $H = R_m - R_c\sin\psi_m$ and that $V = R_c\cos\psi_m$ (See Equations (10) and (11)), Equation (13) becomes*:

$$\sin\psi = (r^2 - R_m^2 + 2R_mR_c\sin\psi_m)/(2rR_c) \tag{13}$$

---

*This expression is seen to be identical to that recorded by Baxter [9].

II. ANALYSIS OF TOOTH PROFILE CHANGES BETWEEN TRANSVERSE PLANES

1. Analytical Development

Consider again the pitch plane of Figure 3. and 6. R_c is the "mean cutter radius." That is, R_c is the distance from C to the tooth surface in the pitch plane. The cutter radius $\hat{r}$ for other points on the tooth surface is a function of the elevation z of those points above or below the pitch plane. For example, for an "inside" tooth surface $\hat{r}$ might be expressed as:

$$\hat{r} = R_c + F(z) \tag{15}$$

where F(z) describes the cutter geometry. In addiiton to X,Y and $\hat{X},\hat{Y}$, let $\hat{\hat{X}},\hat{\hat{Y}}$ be a third coordinate system with origin at the cutter center C and with $\hat{\hat{X}}$ parallel to OP as shown in Figure 7., where P is a typical point along the tooth centerline. Then the angle between $\hat{\hat{X}},\hat{\hat{Y}}$ and $\hat{X},\hat{Y}$ is ε, the small angle between OP and the X axis.

Equation (15) provides a relationship between the cutter radius $\hat{r}$ and the elevation z of a point on the tooth surface. By solving for z the relationship may be expressed in the form:

$$z = f(\hat{r}) \tag{16}$$

The cutter profile, described by the function F(z) of Equation (15), is thus also described by the function $f(\hat{r})$ in Equation (16). However, in Equation (16) the ensuing tooth surface is readily seen to be a surface of revolution. Also, Equation (16) may be viewed as providing as a description of the tooth profile in the normal plane.

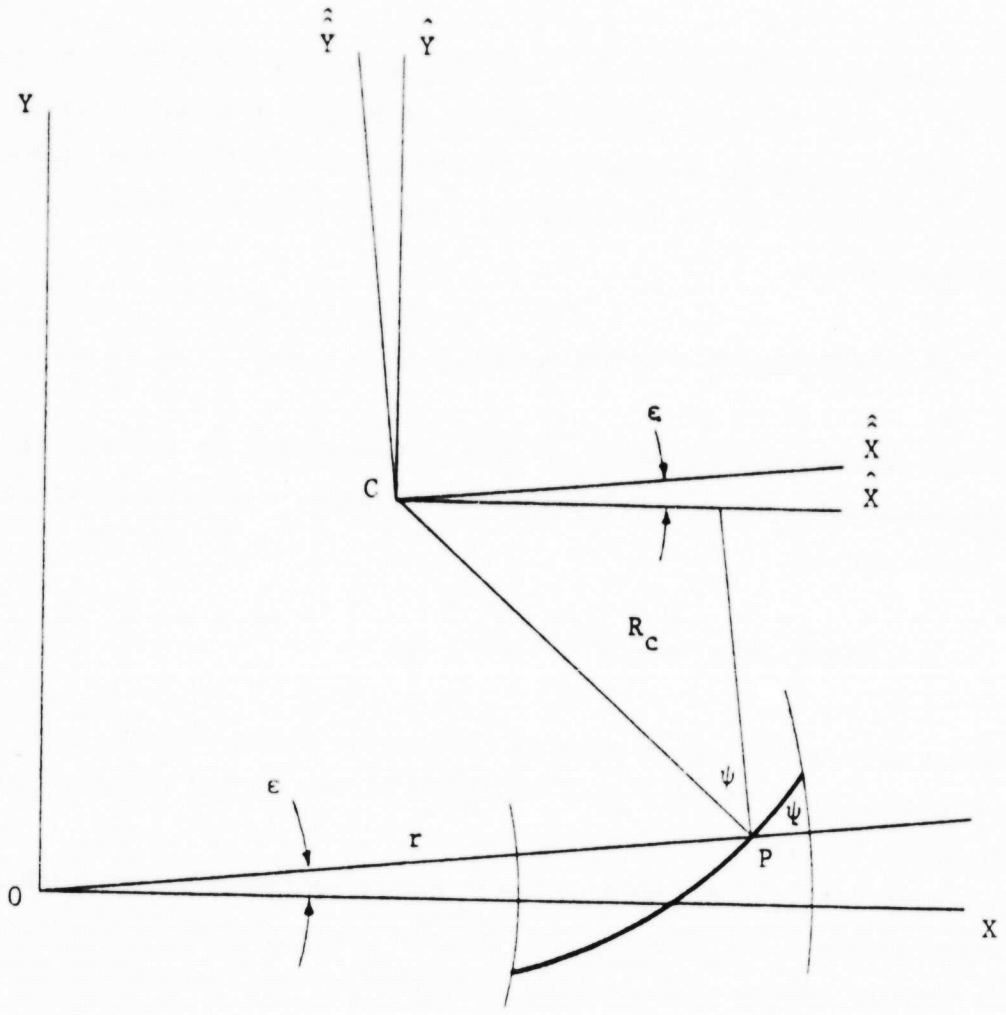

Figure 7. Coordinate Systems in the Pitch Plane

The cutter radius $\hat{r}$ may be expressed in terms of the coordinates $\hat{x},\hat{y}$ and $\hat{\hat{x}},\hat{\hat{y}}$ in the form:

$$\hat{r} = (\hat{x}^2 + \hat{y}^2)^{\frac{1}{2}} = (\hat{\hat{x}}^2 + \hat{\hat{y}}^2)^{\frac{1}{2}} \tag{17}$$

Hence, by comparing Equations (16) and (17) z may be considered to be a function of $\hat{x}$ and $\hat{y}$ or of $\hat{\hat{x}}$ and $\hat{\hat{y}}$. If $\hat{x}$, or $\hat{\hat{x}}$, has a constant value, Equation (16) provides a description of the tooth profile in a <u>transverse</u> plane. For example, if $x = R_c\sin\psi_m$ the tooth profile in the mid-transverse plane is

$$z = f([R_c^2\sin^2\psi_m + \hat{y}^2]^{\frac{1}{2}}) = g(\hat{y}, \psi_m) \tag{18}$$

That is the elevation of a point on the tooth surface in the mid-transverse plane depends upon $\hat{y}$. For a general transverse plane, Equation (18) may be expressed as:

$$z = f([R_c^2\sin^2\psi_m + \hat{\hat{y}}^2]^{\frac{1}{2}}) = g(\hat{y}, \psi_m) \tag{19}$$

Thus, the tooth profile in a general transverse plane depends upon the spiral angle ψ which in turn is a function of the radial distance r, through Equation (14).

Equation (19) can be used to study tooth profile changes between the transverse planes. For example, a comparison of $g(\hat{\hat{y}},\psi)$ with $g(\hat{\hat{y}},\psi_m)$ provides a measure of the modification of the transverse profile from the profile in the mid-transverse plane. Equation (19) is also useful for determining the pressure angle changes between the transverse planes. To see this, consider the profile in the transverse plane depicted in Figure 8. Let θ be the pressure angle and let θ_c be its complement. Then, for the inside tooth surface $\tan\theta_c$ is:

$$\tan\theta_c = \partial z/\partial(-\hat{\hat{y}}) = -(dz/d\hat{r})(\partial\hat{r}/\partial\hat{\hat{y}}) \tag{20}$$

or

$$\tan\theta_c = -f'(\hat{r})\hat{\hat{y}}/\hat{r} \tag{21}$$

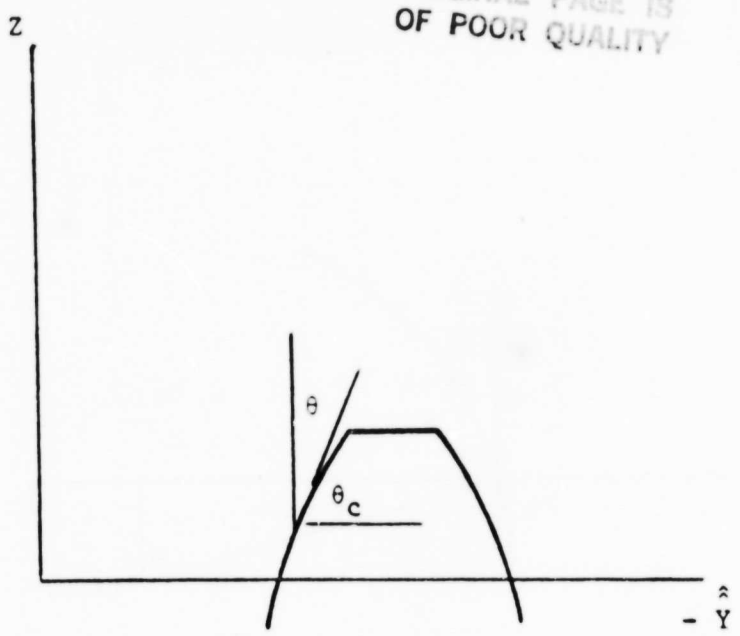

Figure 8. Tooth Profile in the Transverse Plane

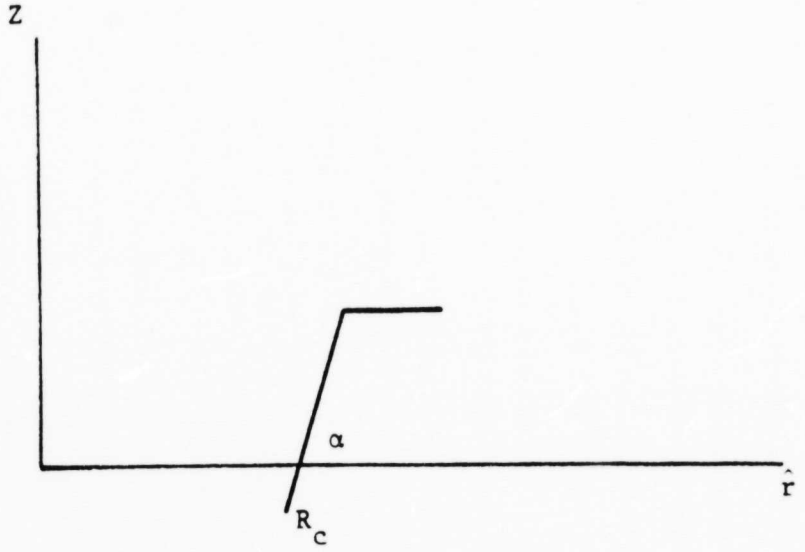

Figure 9. Straight-Line Tooth Profile in the Normal Plane

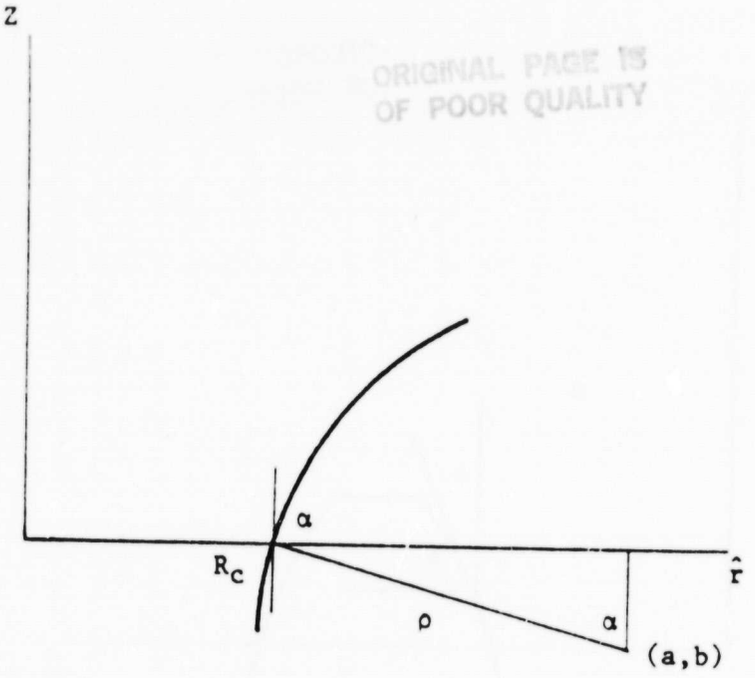

Figure 10. Circular Tooth Profile in the Normal Plane

But since $\tan\theta_c = \cot\theta$, the pressure angle θ (in the transverse plane) is

$$\theta = -\tan^{-1} \hat{r}/f'(\hat{r})\hat{y} \tag{22}$$

Equation (22) may be viewed as an algorithm which provides the pressure angle as a function of the radial distance r from the gear center. Moreover, it is a valid algorithm for any cutter profile.

2. Examples

Equation (22) was used to study the pressure angle changes through the transverse planes along the inside tooth surface, for three cutter profile shapes: 1) a straight line profile, 2) a circular profile, and 3) an involute profile.

1) Straight Line Cutter Profile. Figure 9. depicts a straight line tooth profile in the normal plane. In this case Equation (16) takes the form:

$$z = f(\hat{r}) - (\tan\alpha)(\hat{r} - R_c) \tag{23}$$

where R_c is the mean cutter radius and α is the cutter inclination. By substituting into Equation (22) we obtain the transverse plane pressure angle:

$$\theta = \tan^{-1} (\cot\alpha)\ 1 + (R_c/\hat{y})^2\sin^2\psi\ ^{\frac{1}{2}} \tag{24}$$

where we have replaced $\hat{r}$ by $(R_c^2\sin^2\psi + \hat{y}^2)^{\frac{1}{2}}$ as in Equation (18). The spiral angle ψ may be expressed in terms of the radial distance r by either Equation (13) or (14). Hence, θ is a function of r.

Figure 12. shows a computer drawn graph of θ at the pitch plane level (that is, with $\hat{y} = -R_c\cos\psi$) for R_c = 6.0 in. (15.24 cm), R_m = 7.0 in. (17.78 cm), $\psi_m = 70^o$, and α = 70.

2) Circular Cutter Profile. Figure 10. depicts a circular tooth profile in the normal plane. In this case the equation of the profile may be expressed as:

$$(z - b)^2 + (\hat{r} - a)^2 = \rho^2 \tag{25}$$

where a, b, and ρ are the circle center coordinates and the circle radius as shown in Figure 10. If α is the cutter inclination at the mean cutter radius, then a and b may be expressed as:

$$a = R_c + \rho\sin\alpha \quad \text{and} \quad b = -\rho\cos\alpha \tag{26}$$

Hence, Equation (16) may be expressed in the form:

$$z = f(\hat{r}) = -\rho\cos\alpha + [\rho^2 - (\hat{r} - R_c - \rho\sin\alpha)^2]^{\frac{1}{2}} \tag{27}$$

Then by substituting into Equation (22), we obtain the transverse plane pressure angle:

$$\theta = \tan^{-1} \frac{\{\rho^2 - [(R_c^2\sin^2\psi + \hat{y}^2)^{\frac{1}{2}} - R_c - \rho\sin\alpha]^2\}(R_c^2\sin^2\psi + \hat{y}^2)^{\frac{1}{2}}}{[(R_c^2\sin^2\psi + \hat{y}^2)^{\frac{1}{2}} - R_c - \rho\sin\alpha]\hat{y}} \tag{28}$$

where, as before, we have replaced r by $(R_c^2\sin^2\psi + \hat{y}^2)^{\frac{1}{2}}$.

Figure 12. also shows a graph of Equation (28) for R_c = 6.0 in. (15.24 cm), R_m = 7.0 in. (17.78 cm), ρ = 1.0 in. (2.54 cm), $\psi_m = 30^\circ$, $\alpha = 70^\circ$, and $\hat{y} = -R_c\cos\psi$.

3) Involute Profile. Figure 11. depicts an involute tooth profile in the normal plane, together with the generating circle of the involute. In terms of the ξ,η coordinate system, the coordinates of a typical point P on the involute curve may be expressed as:

$$\xi = \rho(\sin\hat{\theta} - \hat{\theta}\cos\hat{\theta}) \tag{29}$$

and

$$\eta = \rho(\cos\hat{\theta} + \hat{\theta}\sin\hat{\theta}) \tag{30}$$

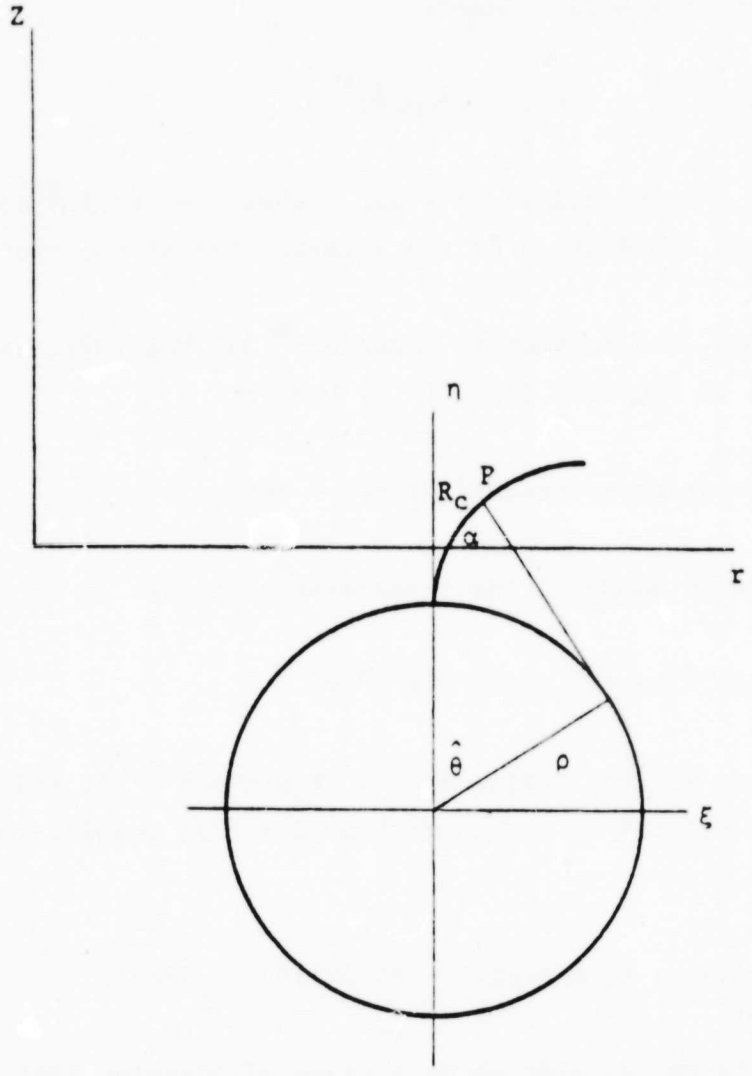

Figure 11. Involute Tooth Profile in the Normal Plane Together with the Involute Generating Circle

where ρ is the radius of the generating circle and $\hat{\theta}$ is the pressure angle in the normal plane. Equations (29) and (30) are parametric equations of the profile with $\hat{\theta}$ being the parameter. In the $z,\hat{r}$ coordinate system these equations may be written as:

$$z = -\eta_0 + \rho(\cos\hat{\theta} + \hat{\theta}\sin\hat{\theta}) \tag{31}$$

and

$$\hat{r} = R_c - \xi_0 + \rho(\sin\hat{\theta} - \hat{\theta}\cos\hat{\theta}) \tag{32}$$

where ξ_0 and η_0 are the values of ξ and η when $\hat{\theta} = (\pi/2)-\alpha$ (that is, ξ_0 and η_0 are the coordinates of the intersection of the profile and the $\hat{r}$-axis).

In this case, the parametric Equations (31) and (32) replace Equation (16). In Equation (22), $f'(\hat{r})$ becomes

$$f'(\hat{r}) = dz/d\hat{r} = (dz/d\hat{\theta})/(d\hat{r}/d\hat{\theta}) = \cot\hat{\theta} \tag{33}$$

Hence, the pressure angle in the transverse plane is:

$$\theta = \tan^{-1}[\tan\hat{\theta}(r_c^2\sin^2\psi + \hat{y}^2)^{1/2}/\hat{y}] \tag{34}$$

where, as before, we have replaced $\hat{r}$ by $(R_c^2\sin^2\psi + \hat{y}^2)^{1/2}$, and where in this case, $\hat{y}$ is related to $\hat{\theta}$ through Equation (32) leading to the expression:

$$\hat{y} = -\{[R_c - \xi_0 + \rho(\sin\hat{\theta} - \hat{\theta}\cos\hat{\theta})]^2 - R_c\sin^2\psi\}^{1/2} \tag{35}$$

Finally, Figure 12. also shows a graph of Equation (34) for R_c = 6.0 in. (15.24 cm), R_m = 7.0 in. (17.78 cm), = 7.0 in. (17.78 cm), ψ_m = 30, $\hat{\theta}$ = 20°, and $\hat{y}$ given by Equation (35).

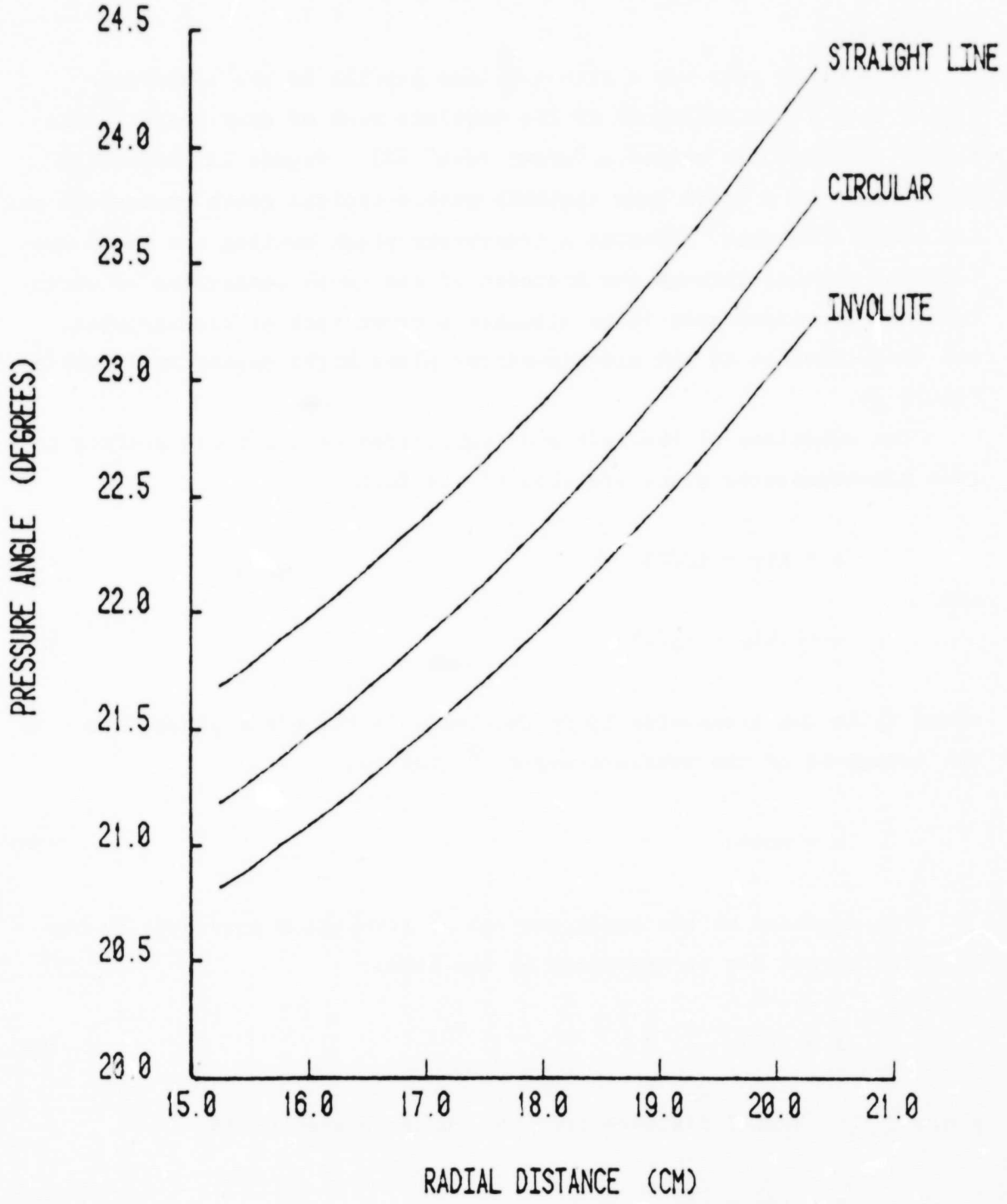

Figure 12. Transverse Plane Pressure Angle Variation for Three Cutter Profiles.

III. DETERMINATION OF CUTTER PROFILE FOR A STRAIGHT LINE TOOTH PROFILE IN THE TRANSVERSE PLANE

1. Analysis

If a crown gear has a straight line profile in the transverse plane, then it is analogous to the involute rack of spur gears. Such a gear is sometimes called a "crown rack" [7]. Figure 13. shows the pitch plane of a crown gear together with a typical tooth centerline and the coordinate axes. Imagine a transverse plane cutting the tooth surface and passing through the midpoint of the tooth centerline as shown. Then, if the crown gear is to simulate a crown rack at its midpoint, the tooth profile in the mid-transverse plane might appear as shown in Figure 14.

The equations of the left and right sides of the tooth surface in this mid-transverse plane are then of the form:

$$z = k(y + t_0/2) \tag{36}$$

and

$$z = -k(y - t_0/2) \tag{37}$$

where t_0 is the transverse tooth thickness in the pitch plane, and k is the cotangent of the pressure angle θ, that is,

$$k = \cot\theta \tag{38}$$

The equation of the tooth surface of revolution generated by the circular cutter can be expressed in the form:

$$\hat{z} = f(\hat{r}) \tag{39}$$

where $\hat{r}$, the radial distance from the cutter center C, is

$$\hat{r} = (\hat{x}^2 + \hat{y}^2)^{\frac{1}{2}} \tag{40}$$

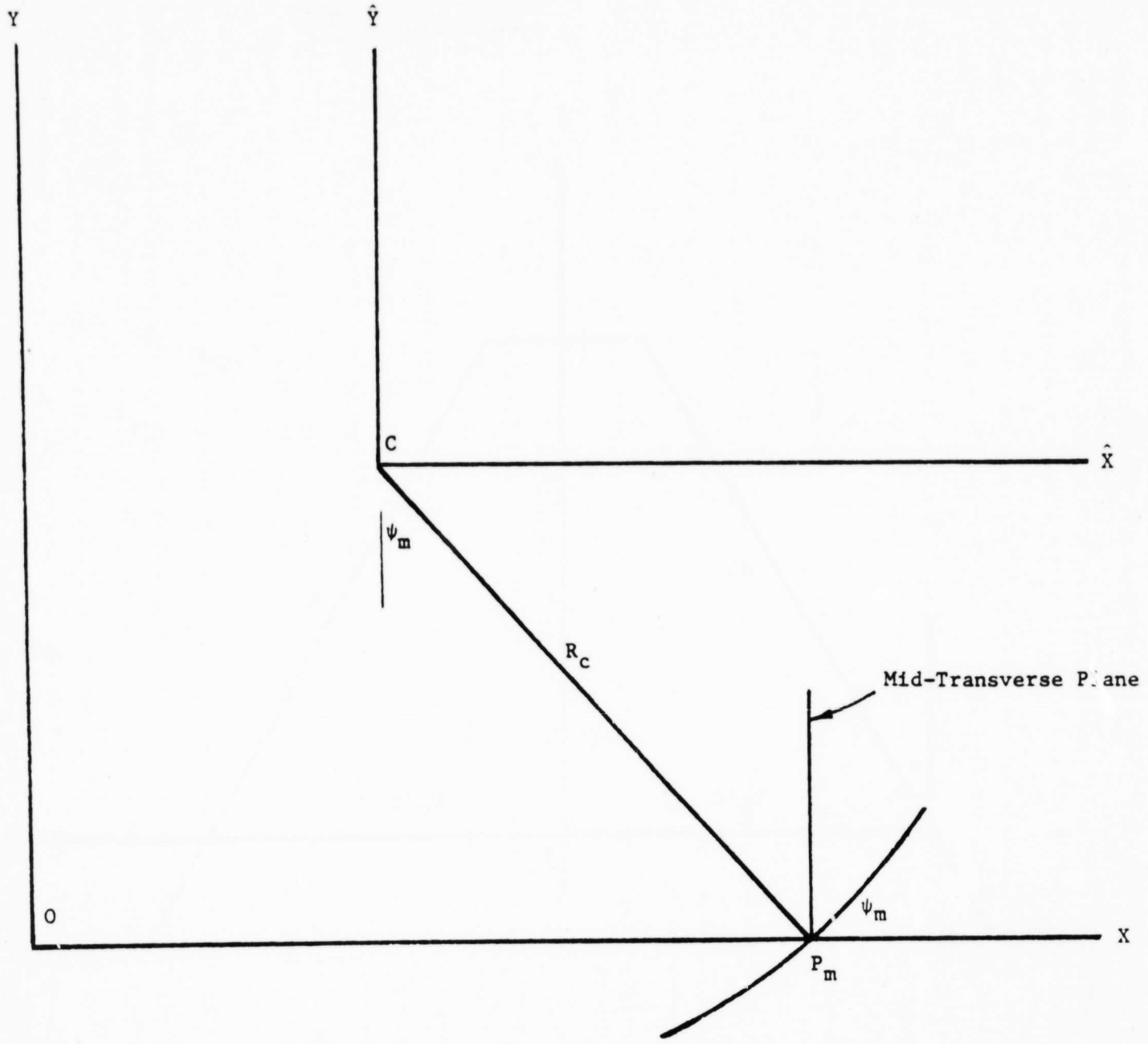

Figure 13. Pitch Plane of Circular Cut Crown Gear.

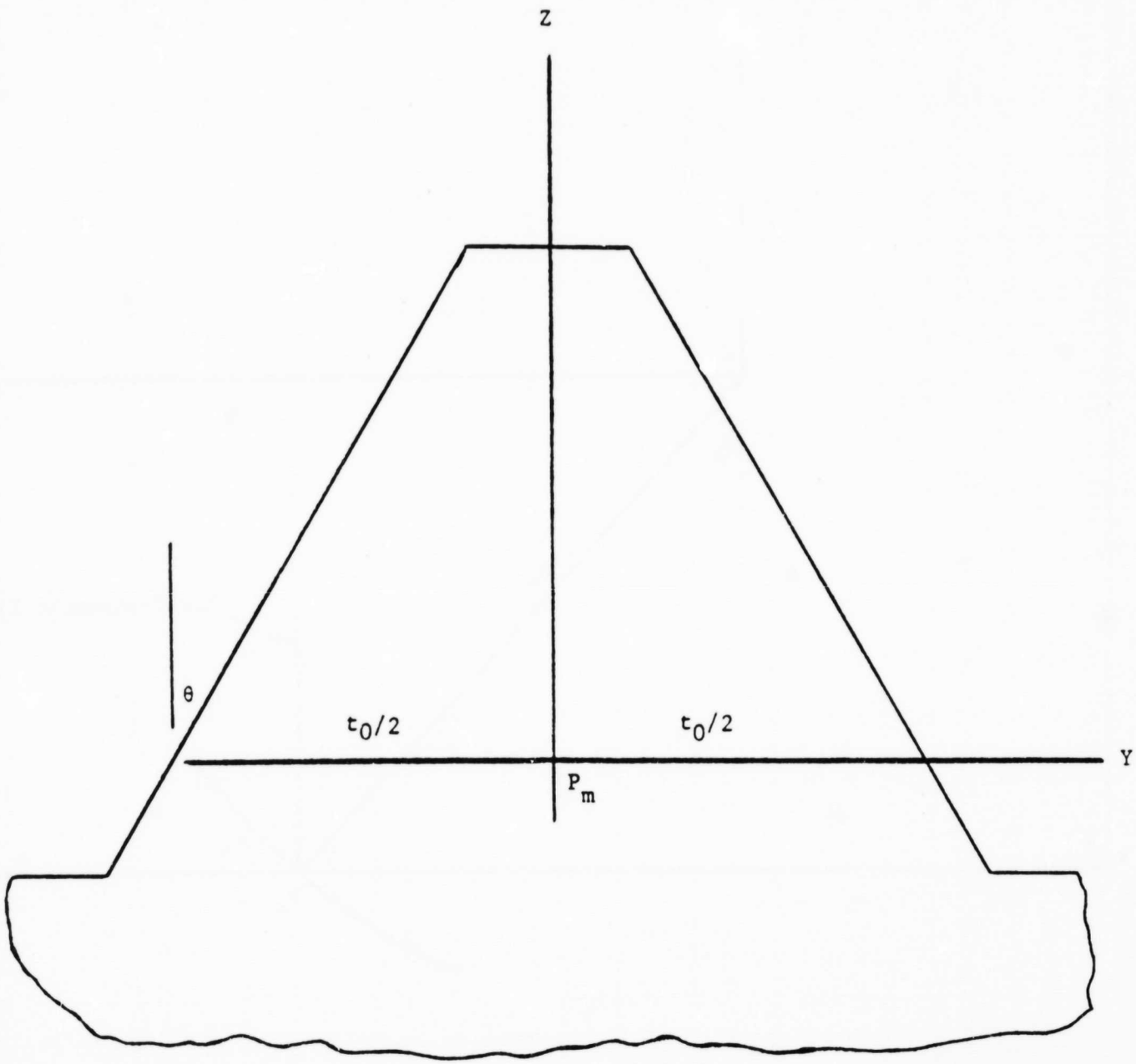

Figure 14. Tooth Profile of Crown Rack in the Mid Transverse Plane.

The equation of the mid-transverse cutting plane as shown in Figure 13. is simple:

$$\hat{x} = R_c \sin\psi_m \tag{41}$$

When $\hat{x}$ has the value $R_c\sin\psi_m$, $f(\hat{r})$ as determined by Equations (40) and (41), has the form of Equations (36) or (37) for a straight line profile in the mid-transverse plane. By substituting from Equation (41) into (40) and by solving for $\hat{y}$ leads to:

$$\hat{y} = -(\hat{r}^2 - R_c^2\sin^2\psi_m)^{\frac{1}{2}} \tag{42}$$

where the negative root is taken since y is negative (See Figure 14.). Hence, from Equations (1), (36), (37), (38), (39), $f(\hat{r})$ takes the form:

$$f(\hat{r}) = [V + (t_0/2) - (\hat{r}^2 - R_c^2\sin^2\psi_m)^{\frac{1}{2}}]\cot\theta \tag{43}$$

or

$$f(\hat{r}) = [-V + (t_0/2) + (\hat{r}^2 - R_c^2\sin^2\psi_m)^{\frac{1}{2}}]\cot\theta \tag{44}$$

where Equation (43) corresponds to the left or "outside" tooth surface and Equation (44) corresponds to the right or "inside" tooth surface. It is easily shown that these surfaces of revolution are hyperboloids. (See Section 2. of the Appendix.)

2. Numerical Results

In Equation (43) and (44), if $\hat{x} = R_c\sin\psi_m$ in $\hat{r}$, then f(r) becomes $[V + (t_0/2) + \hat{y}]\cot\theta$ or $[-V + (t_0/2) - \hat{y}]\cot\theta$ depending upon whether f(r) describes an "outside" or "inside" tooth surface. As expected, these expressions match those of the straight line profiles in the mid-transverse plane.) If however, in Equations (43) and (44), $\hat{x} = R_c\sin\psi$, that is, if $\psi \neq \psi_m$, then the transverse tooth profiles are no longer straight but instead they are described by the expressions:

$$z = [V + (t_0/2) - (R_c^2 \sin^2\psi + y^2 - R_c^2 \sin^2\psi_m)^{1/2}]\cot\theta \qquad (45)$$

and

$$z = [-V + (t_0/2) + (R_c^2 \sin^2\psi + y^2 - R_c^2 \sin^2\psi_m)^{1/2}]\cot\theta \qquad (46)$$

Equations (45) and (46) may be used to obtain a numerical analysis of the transverse tooth profile change along the centerline. That is, by using Equation (13) or Equation (14) the variation of z with $\hat{y}$ (transverse distance) and with r (radial distance) is determined if the cutter settings and cutter radius are known.

Such numerical calculations were performed for a crown gear with a cutter radius R_c of 6.0 in. (152.4 mm) horizontal and vertical cutter settings, H and V of 4.0 in. (101.6 mm) and $3\sqrt{3}$ in. (131.98 mm), and mid-spiral angle ψ_m of 30^o, and a pressure angle ψ_m at the mid transverse plane of 20^o. Also, the inner and outer gear radii were taken as 6.0 in. (152.4 mm) and 8.0 in. (203.2 mm). (The data are also the same as those used in the gear depicted in Figure 5.)

These calculations were performed for the left or "outside" tooth surface. The results are shown in Figures 15. to 18. where the pressure angle is plotted as a function of the radial distance, the vertical coordinate, and the transverse coordinate.

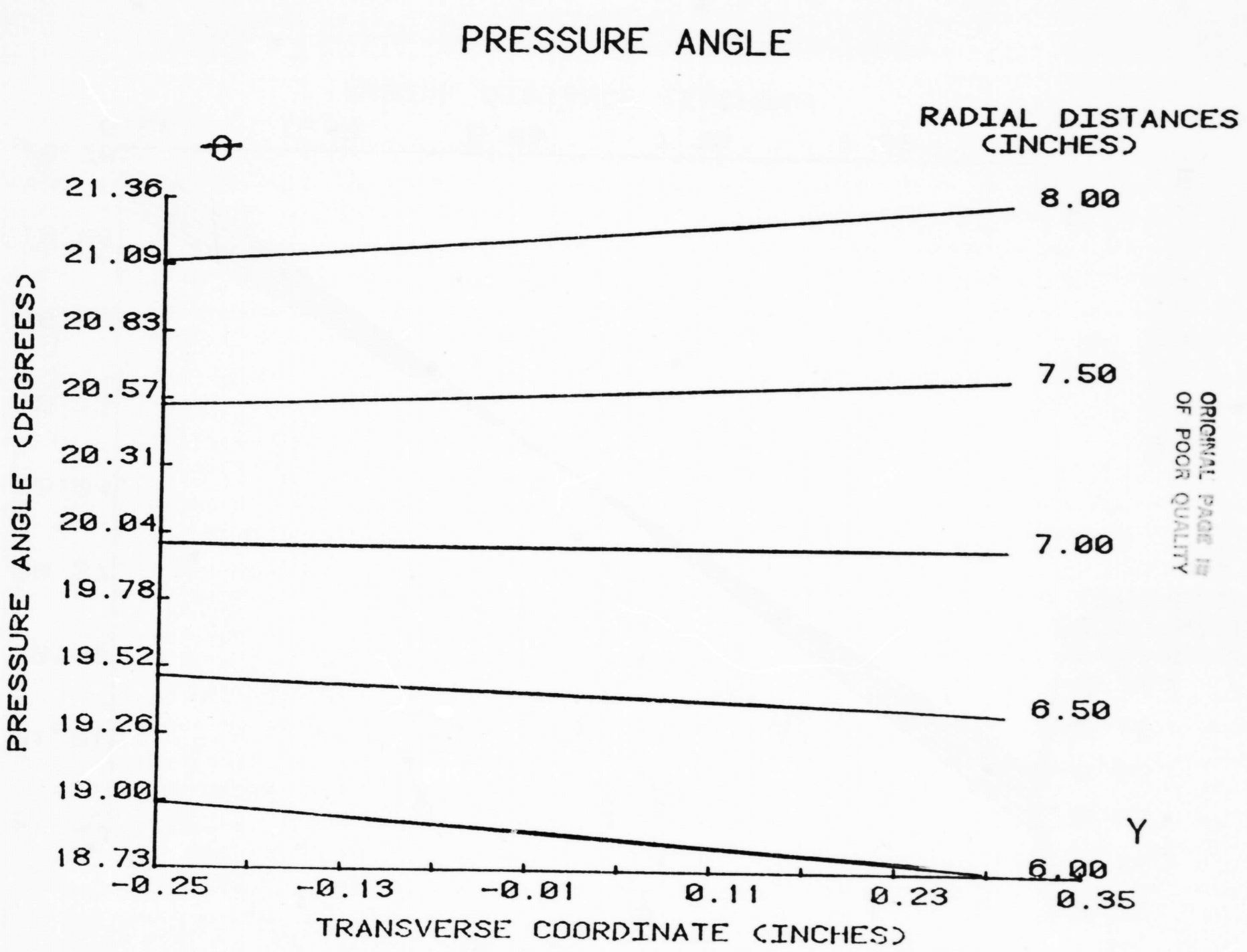

Figure 15. Variation of the Pressure Angle with the Transverse Coordinate.

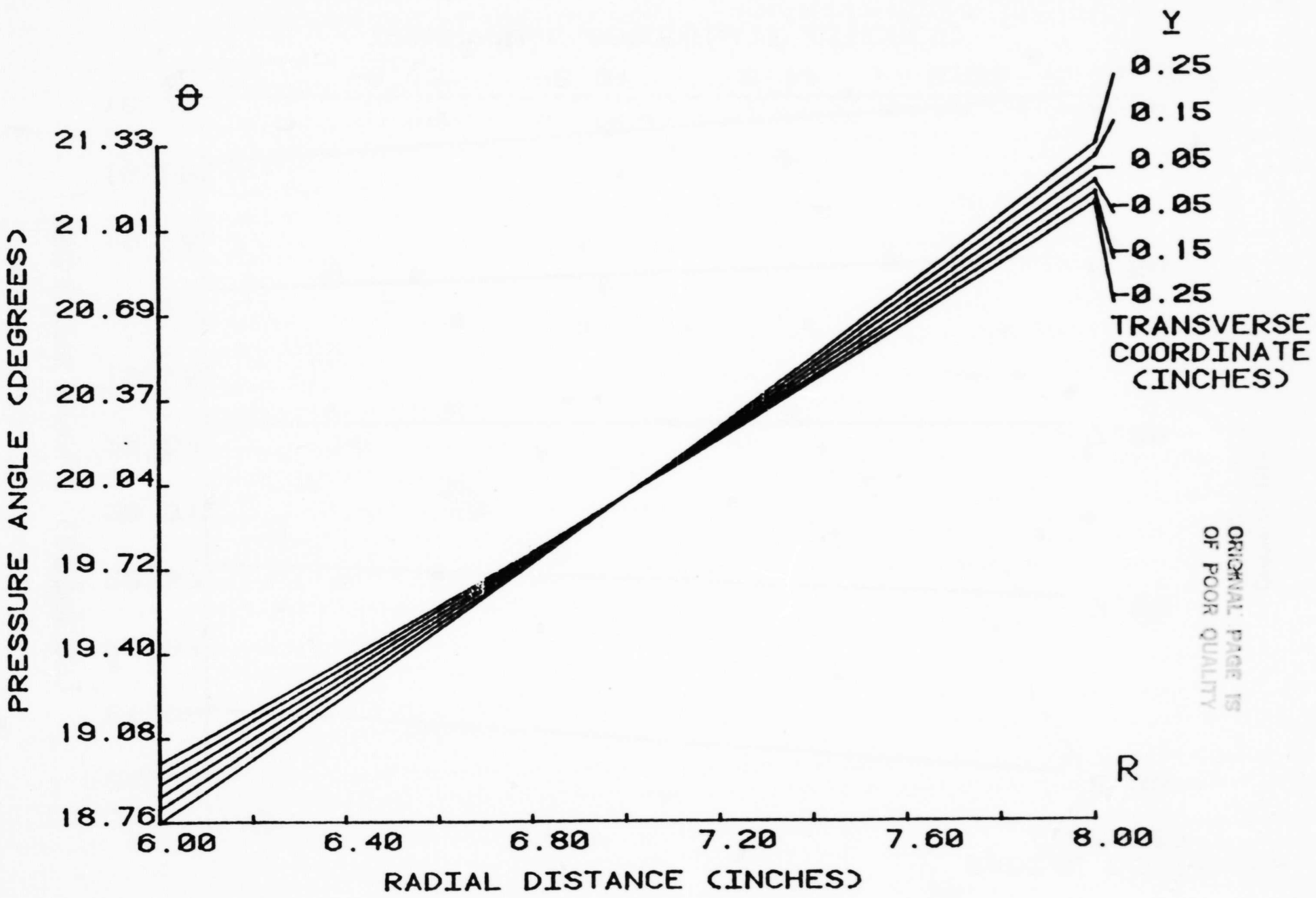

Figure 16. Variation of the Pressure Angle with the Radial Distance.

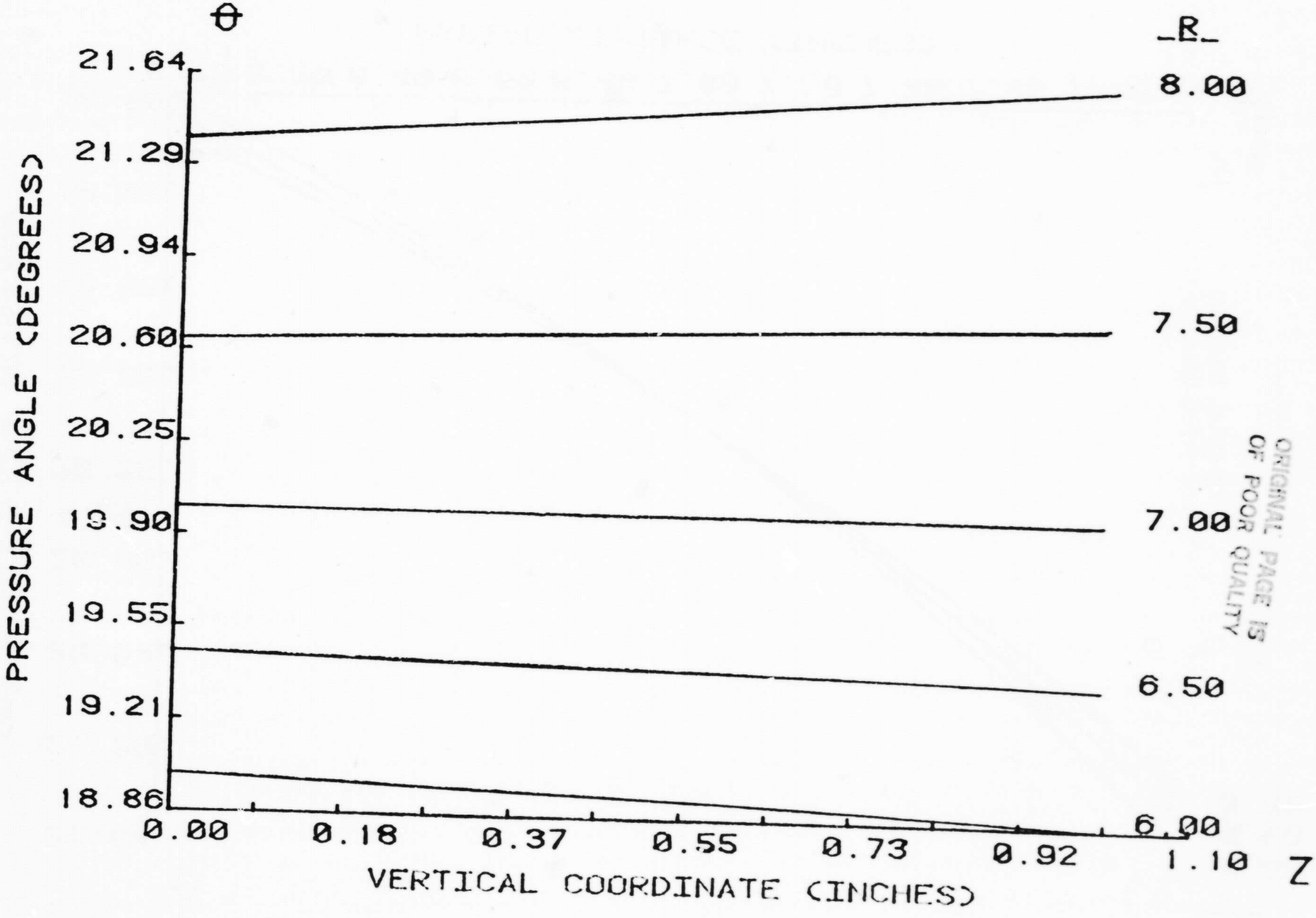

Figure 17. Variation of the Pressure Angle with the Vertical Coordinate.

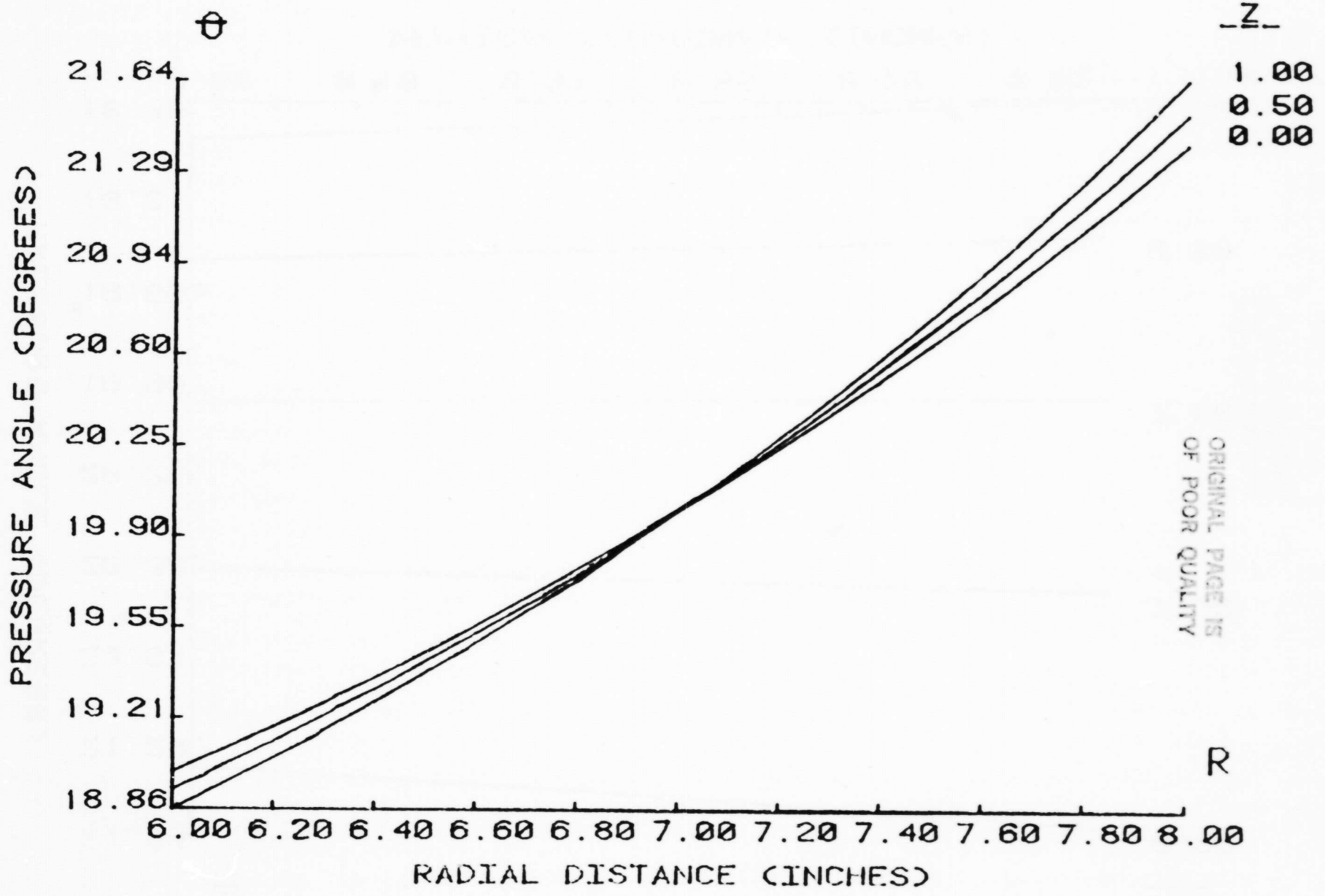

Figure 18. Variation of the Pressure Angle with the Radial Distance.

IV. RADII OF CURVATURE OF CIRCULAR-CUT TOOTH SURFACES

Knowledge of the principal radii of curvature of a gear tooth surface is a point of departure for the study of contact stresses, lubrication, wear, fatigue, and life. In the following paragraphs procedures for finding these radii of curvature are provided for circular-cut spiral bevel crown gears.

1. Differential Geometry Formulae

Since the principal radii of curvature of a gear tooth surface at a point are among the major factors affecting the lubrication, surface fatigue, contact stress, wear and life of the gear, it is helpful to summarize the basic formulae from elementary differential geometry which may be used to determine thse radii of curvature.

Suppose a surface S is defined by a pair of parameters u^1 and u^2 through the vector parametric equation $\underset{\sim}{P} = \underset{\sim}{P}(u^1, u^2)$ where $\underset{\sim}{P}$ is the position vector of a typical point P on S. Then base vectors $\underset{\sim}{e}_i (i = 1,2)$ tangent to S at P are given by

$$\underset{\sim}{e}_i = \partial \underset{\sim}{P} / \partial u^i \tag{47}$$

A surface metric tensor $g_{ij}(i,j = 1,2)$ may then be defined as

$$g_{ij} = \underset{\sim}{e}_i \cdot \underset{\sim}{e}_j \tag{48}$$

Let g be the determinant of g_{ij}. Then it is easily shown that

$$g = |\underset{\sim}{e}_1 \times \underset{\sim}{e}_2| \tag{49}$$

Hence, a unit vector $\underset{\sim}{n}$ normal to S is then

$$\underset{\sim}{n} = \underset{\sim}{e}_1 \times \underset{\sim}{e}_2 / g \tag{50}$$

Let the fundamental vector $\underset{\sim}{h}_i (i = 1,2)$ be defined as

$$\underset{\sim}{h}_i = \partial \underset{\sim}{n} / \partial u^i \tag{51}$$

Then, the second fundamental tensor $h_{ij}(i,j = 1,2)$ is defined as

$$h_{ij} = -\underset{\sim}{h}_i \cdot \underset{\sim}{e}_j \tag{52}$$

Letting h be the determinant of h_{ij}, the Gaussian curvature K is defined as

$$K = h/g \tag{53}$$

Let $k_{ij}(i,j = 1,2)$ be defined as

$$k_{ij} = g^{-1}_{i\ell} h_{\ell j} \tag{54}$$

where g^{-1}_{ij} is the inverse of g_{ij}. (Regarding notation, repeated indices represent a sum (that is, from 1 to 2) over that index.) The mean curvature J is then defined as

$$J = k_{\ell\ell} \tag{55}$$

Finally, maximum and minimum radii of curvature R_{max} and R_{min} are then easily calculated in terms of J and K as:

$$R_{max},\ R_{min} = 2/[J^2 \pm (J^2 - 4K)^{\frac{1}{2}}] \tag{56}$$

2. Surface of Revolution

The tooth surface of a circular cut spiral bevel crown gear is a "surface of revolution." That is, it can be developed by rotating a curve in the shape of the cutter profile, about a fixed axis. Consider, for example, the curve C shown in Figure 19. If C is rotated about the Z-axis, it generates a surface of revolution S, a portion of which can be considered as the surface of a circular cut spiral bevel crown gear. Let C be defined by the expression:

$$z = f(r) \tag{57}$$

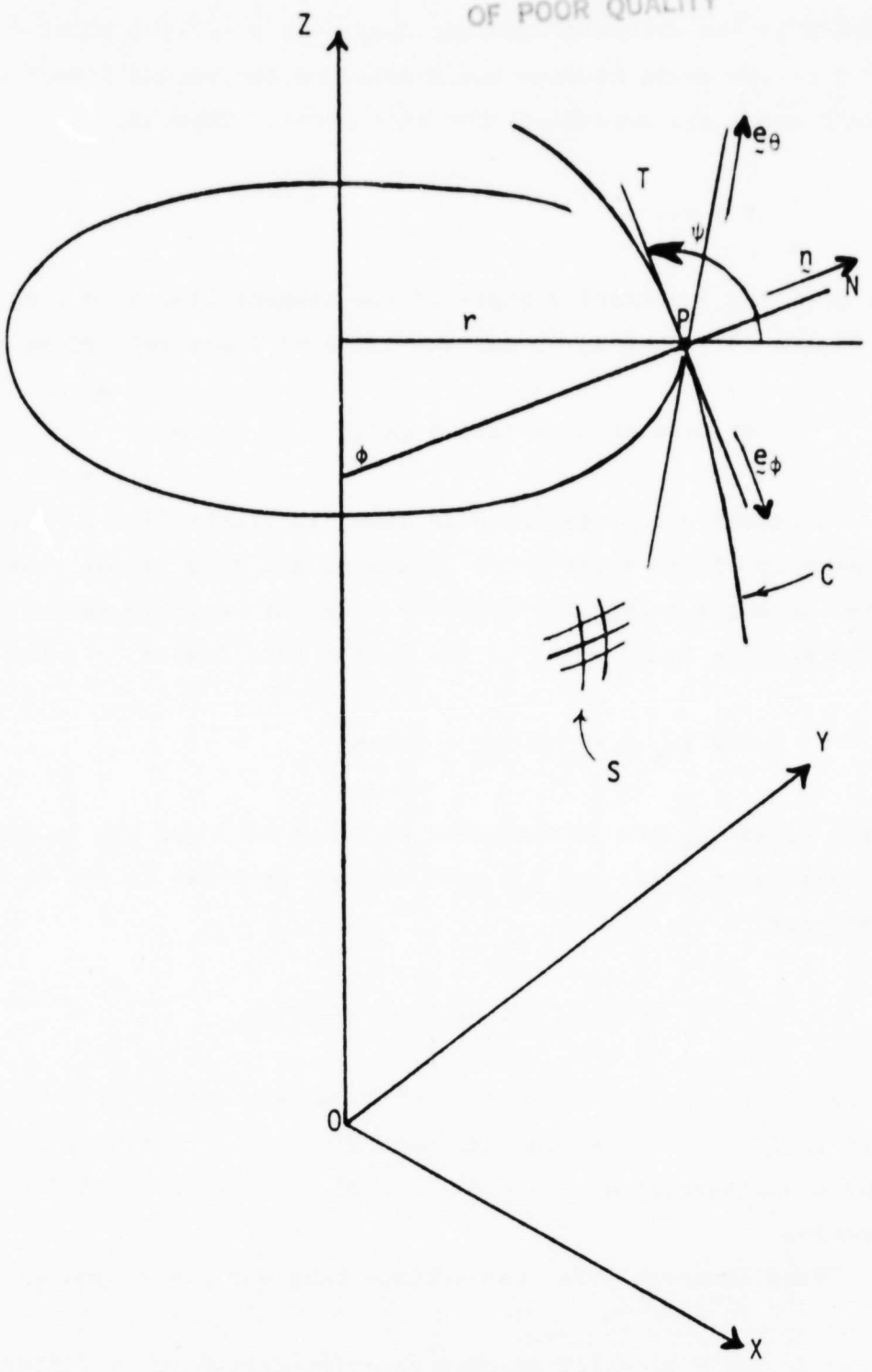

Figure 19. A Surface of Revolution About the Z-Axis

where r is the distance from the Z-axis to a typical point P on C. Let ϕ be the angle between the Z-axis and the normal line N of S at P. Then r and ϕ are dependent upon each other. That is,

$$r = r(\phi) \tag{58}$$

Let ψ be the inclination angle of the tangent line T to C at P as shown in Figure 19. Then ψ, ϕ, and the slope of T are related as follows:

$$dz/dr = df/dr = \tan\psi = \tan(\pi - \psi) = -\tan\phi \tag{59}$$

Consider a top view of S as shown in Figure 20. In this view P is seen to lie on a circle of radius r, and on a radial line R which makes an angle θ with the X-axis. Then the position vector $\underset{\sim}{P}$ of P relative to 0, a fixed point on the Z-axis (See Figure 19.) is:

$$\underset{\sim}{P} = z\underset{\sim}{n}_z + r\underset{\sim}{n}_r = r\underset{\sim}{n}_r + f(r)\underset{\sim}{n}_z \tag{60}$$

where $\underset{\sim}{n}_r$ and $\underset{\sim}{n}_z$ are unit vectors parallel to R and the Z-axis. Hence, in terms of $\underset{\sim}{n}_x$, $\underset{\sim}{n}_y$, and $\underset{\sim}{n}_z$, unit vectors parallel to the X, Y, and Z axes, $\underset{\sim}{P}$ becomes:

$$\underset{\sim}{P} = r\cos\theta\ \underset{\sim}{n}_x + r\sin\theta\ \underset{\sim}{n}_y + f(r)\underset{\sim}{n}_z \tag{61}$$

Since $r = r(\phi)$, P is a function of ϕ and θ . Therefore, it is convenient to let ϕ and θ be the parameters u^1 and u^2 defining S in the parametric representation $\underset{\sim}{P} = \underset{\sim}{P}(u^1, u^2)$ of the foregoing differential geometry formulae.

From Equation (47), the surface base vectors $\underset{\sim}{e}_1$ and $\underset{\sim}{e}_2$ become:

$$\underset{\sim}{e}_1 = \underset{\sim}{e}_\phi = (dr/d\phi)\cos\theta\ \underset{\sim}{n}_x + (dr/d\phi)\sin\theta\ n_y + (df/dr)(dr/d\phi)\underset{\sim}{n}_z \tag{62}$$

and

$$\underset{\sim}{e}_2 = \underset{\sim}{e}_\theta = -r\sin\theta\ \underset{\sim}{n}_x + r\cos\theta\ \underset{\sim}{n}_y \tag{63}$$

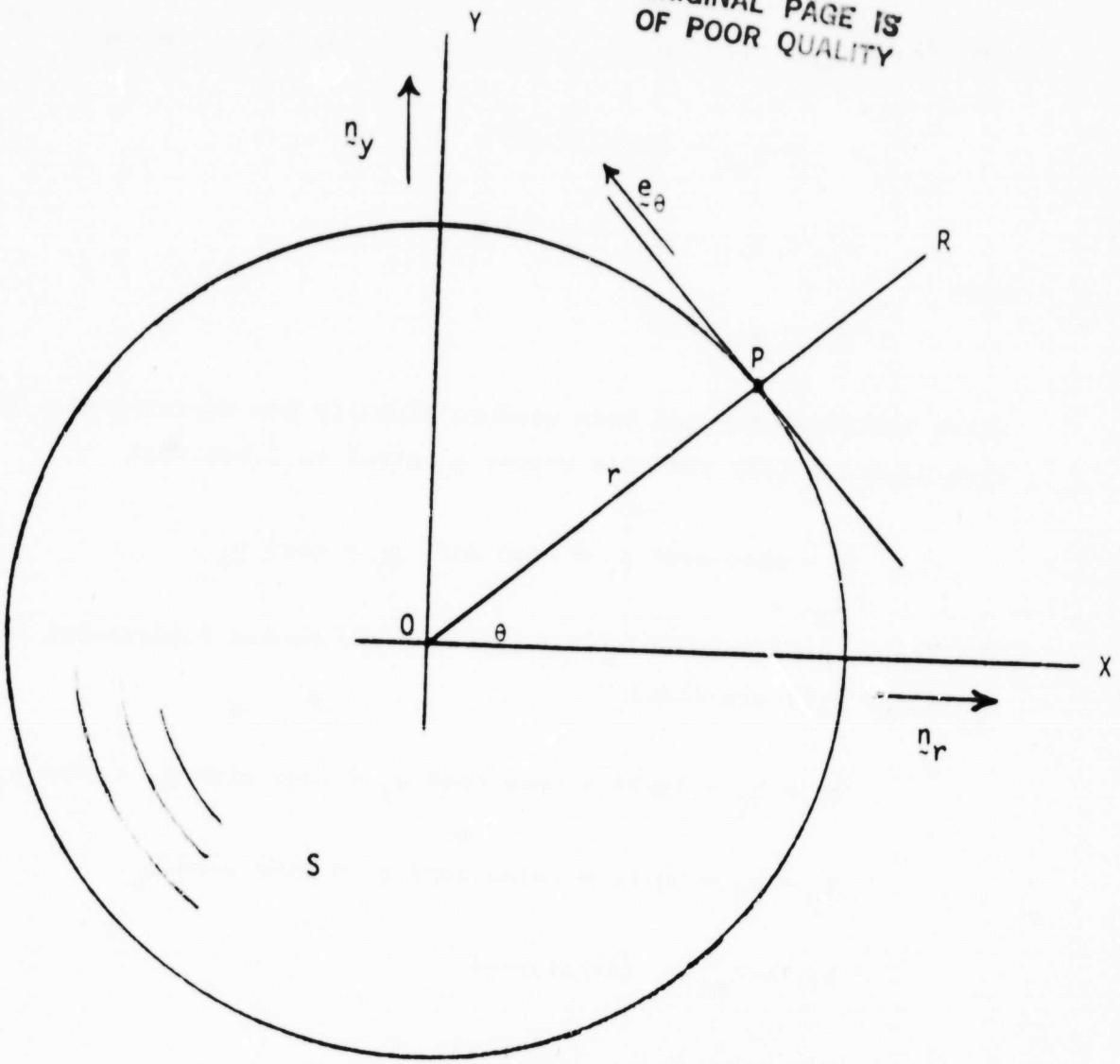

Figure 20. Top View of a Surface of Revolution.

Then, from Equation (48) the metric tensor components become:

$$g_{11} = g_{\phi\phi} = (dr/d\phi)^2 \sec^2\phi \tag{64}$$

$$g_{12} = g_{21} = g_{\phi\theta} = g_{\theta\phi} = 0 \tag{65}$$

and

$$g_{22} = g_{\theta\theta} = r^2 \tag{66}$$

where Equation (59) has been used to simplify the expressions. Hence, from Equation (58) the unit vector $\underset{\sim}{n}$ normal to S becomes:

$$\underset{\sim}{n} = \sin\phi \cos\theta\ \underset{\sim}{n}_x + \sin\phi \sin\theta\ \underset{\sim}{n}_y + \cos\phi\ \underset{\sim}{n}_z \tag{67}$$

The fundamental vectors $h_i (i = \phi,\theta)$ and the second fundamental tensor $h_{ij} (i,j = \phi,\theta)$ are then:

$$\underset{\sim}{h}_1 = \underset{\sim}{h}_\phi = \partial\underset{\sim}{n}/\partial\phi = \cos\phi \cos\theta\ \underset{\sim}{n}_x + \cos\phi \sin\theta\ \underset{\sim}{n}_y - \sin\phi\ \underset{\sim}{n}_z \tag{68}$$

$$\underset{\sim}{h}_2 = \underset{\sim}{h}_\theta = \partial\underset{\sim}{n}/\partial\theta = -\sin\phi \sin\theta\ \underset{\sim}{n}_x + \sin\phi \cos\theta\ \underset{\sim}{n}_y \tag{69}$$

$$h_{11} = h_{\phi\phi} = -(dr/d\phi)\sec\phi \tag{70}$$

$$h_{12} = h_{21} = h_{\phi\theta} = h_{\theta\phi} = 0$$

and

$$h_{22} = h_{\theta\theta} = -r \sin\phi \tag{72}$$

From Equations (53) and (55) the Gaussian curvature and the mean curvature become:

$$K = (\sin\phi \cos\phi)/r(d\phi/dr) \tag{73}$$

and

$$J = -[(\cos\phi)/(dr/d\phi) - (\sin\phi)/r] \tag{74}$$

Finally, using Equation (56) the principal surface radii of curvature become:

$$R_{max} = |(dr/d\phi)/\cos\phi| \tag{75}$$

and

$$R_{min} = |r/\sin\phi| \tag{76}$$

These expressions may be expressed in terms of f by using Equation (59). That is, since

$$\phi = \tan^{-1}(df/dr) \tag{77}$$

then $(d\phi/dr)$ becomes

$$d\phi/dr = -(d^2f/dr^2)/[1 + (df/dr)^2] \tag{78}$$

and hence, R_{max} and R_{min} become:

$$R_{max} = |[1 + (df/dr)^2] / [(d^2f/dr^2)\cos(\tan^{-1}(df/dr))]| \tag{79}$$

and

$$R_{min} = |r/\sin(\tan^{-1}(df/dr))| \tag{80}$$

3. Example

1) An Involute Cutter Profile. Perhaps the most fundamental and theoretically satisfying of all the gear tooth shapes is that generated by an involute curve. Although it may not be practical to generate a spiral bevel gear tooth surface with a rotating cutter in the shape of an involute curve, it is nevertheless informative, as a first illustration, to examine the surface of revolution formed by an involute curve.

Consider the involute curve C as shown in Figure 21. It is convenient to think of C as being generated by "unwrapping" the tangent to the circle. Then the radius of curvature ρ of C at a typical point P is simply the length TP. It is easily seen that ρ is one of the prin-

cipal radii of curvature of the surface of revolution which is obtained by revolving C about the Z-axis in Figure 3.

To see this, consider using Equations (75) and (76) of the foregoing analysis. These equations require knowledge of the radial distance r as a function of the angle (See Figure 3.). To obtain $r(\phi)$ let O be that point on the Z-axis which is at the same elevation as O_c the center of the circle generating C. Then r may be expressed as:

$$r = \underset{\sim}{n}_r \cdot \underset{\sim}{OP} \tag{81}$$

The vector $\underset{\sim}{OP}$ may be written as (See Figure 21.):

$$\underset{\sim}{OP} + \underset{\sim}{OO}_c + \underset{\sim}{O}_c\underset{\sim}{T} + \underset{\sim}{TP} \tag{82}$$

$$\underset{\sim}{OP} = b\underset{\sim}{n}_r + a\underset{\sim}{n}_c - a\phi_c\underset{\sim}{n}_t \tag{83}$$

where b is the distance OO_c, a is the circle radius and ϕ_c is the complement of ϕ. In terms of $\underset{\sim}{n}_r$ and $\underset{\sim}{n}_z$, $\underset{\sim}{OP}$ may be written as:

$$\underset{\sim}{OP} = b - a\cos\phi + a(\pi/2 - \phi)\sin\phi\ \underset{\sim}{n}_r + a\sin\phi + a(\pi/2 - \phi)\cos\phi\ \underset{\sim}{n}_z \tag{84}$$

Hence, from Equation (81) r and $dr/d\phi$ become:

$$r = b - a\cos\phi + a(\pi/2 - \phi)\sin\phi \tag{85}$$

and

$$dr/d\phi = a(\pi/2 - \phi)\cos\phi \tag{86}$$

Therefore, from Equations (75) and (76) the principal radii of curvature of the generated surface of revolution are:

$$R_{max} = b\csc\phi = a\cot\phi + a(\pi/2 - \phi) \tag{87}$$

and

$$R_{min} = a(\pi/2 - \phi) \tag{88}$$

An examination of Figure 21. shows that these expressions can be interpreted simply as:

$$R_{max} = |\underset{\sim}{QP}| \tag{89}$$

and

$$R_{min} = |\underset{\sim}{TP}| \tag{90}$$

Finally, it is interesting to observe that if the same analysis is carried out for an involute curve generated in the opposite direction as in Figure 22. the corresponding surface of revolution has the principal radii of curvature:

$$R_{max} = |\underset{\sim}{QP}| \tag{91}$$

and

$$R_{min} = |\underset{\sim}{TP}| \tag{92}$$

These results are, of course, identical to Equations (89) and (90). However, in this case, the centers of curvature are on opposite sides of the surface.

2) Straight Line Cutter Profile. Consider next a rotating gear tooth cutter with a straight line profile which forms a gear tooth surface with a straight line profile in the normal plane as shown in Figures 23. and 24. Viewed as a surface of revolution, this is a cone. Its defining equation may be expressed as:

$$z = (r - R_c) \cot\theta \tag{93}$$

where θ is the pressure angle as shown in Figure 24. and R_c is the cutter radius at the base of the tooth. From this expression dz/dr and d^2z/dr^2 are readily obtained as:

$$dz/dr = \cot\theta = \tan\phi \tag{94}$$

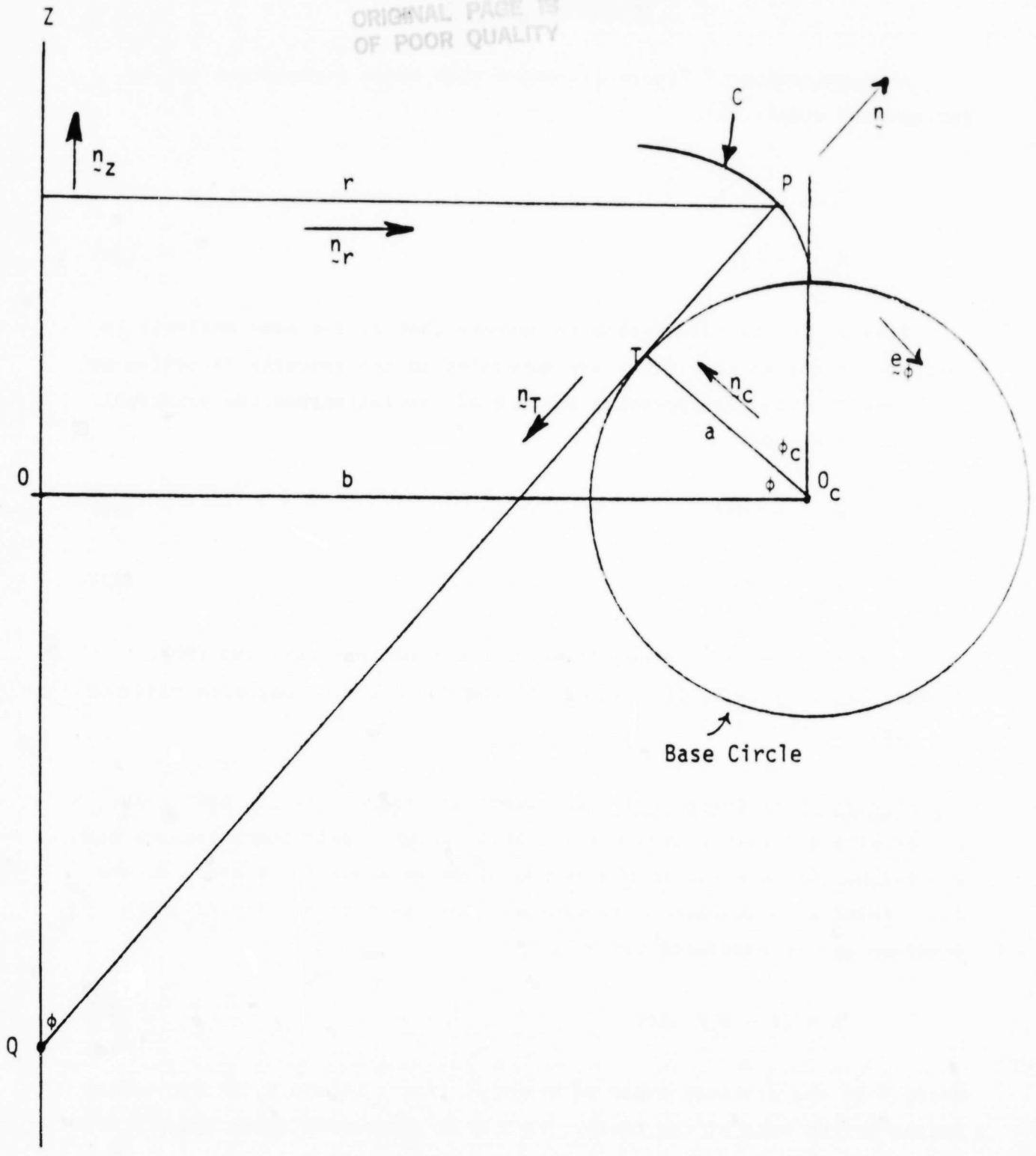

Figure 21. An Involute Curve as a Generator for a Surface of Revolution.

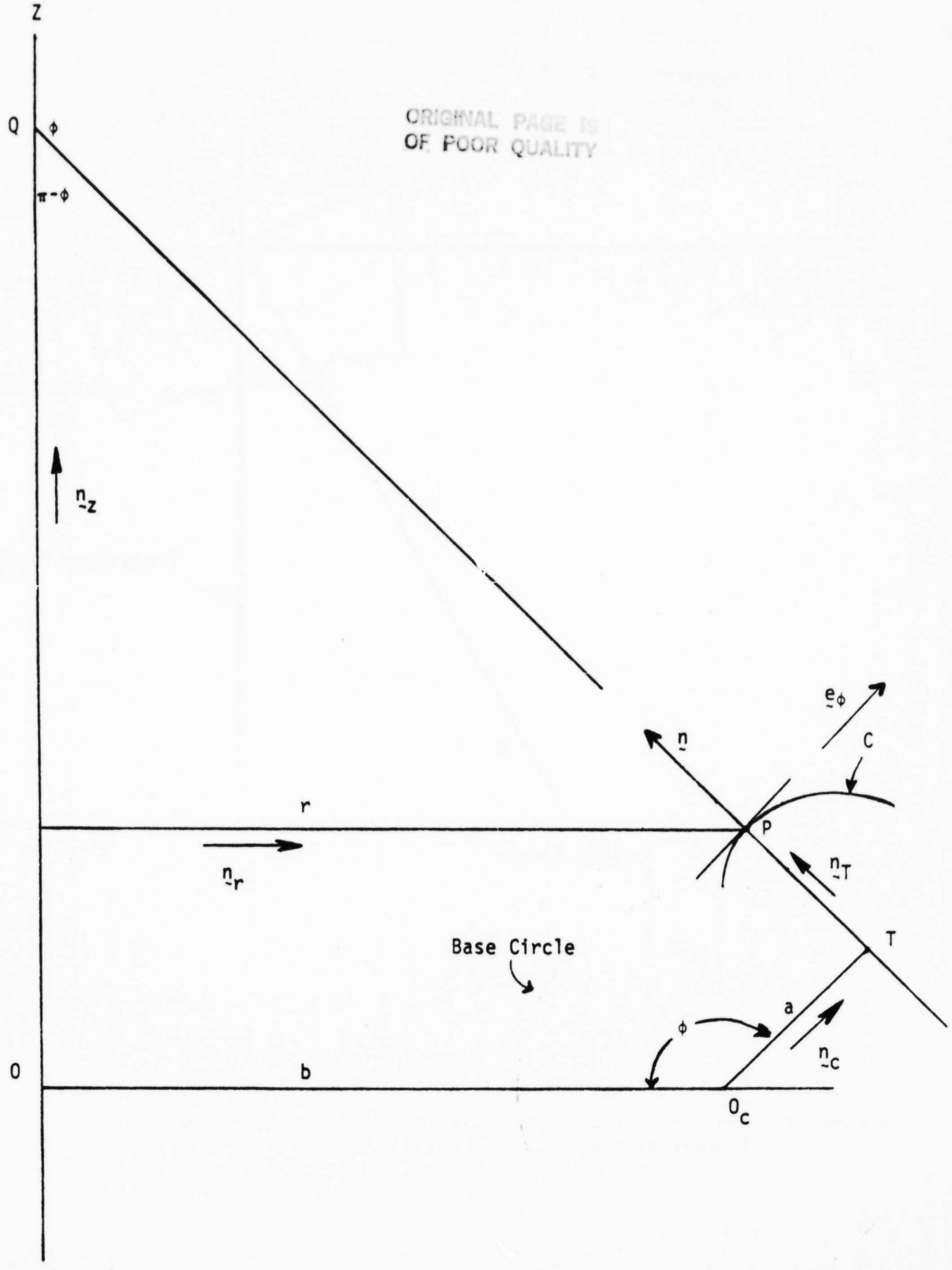

Figure 22. A Second Involute Curve as a Generator for a Surface of Revolution.

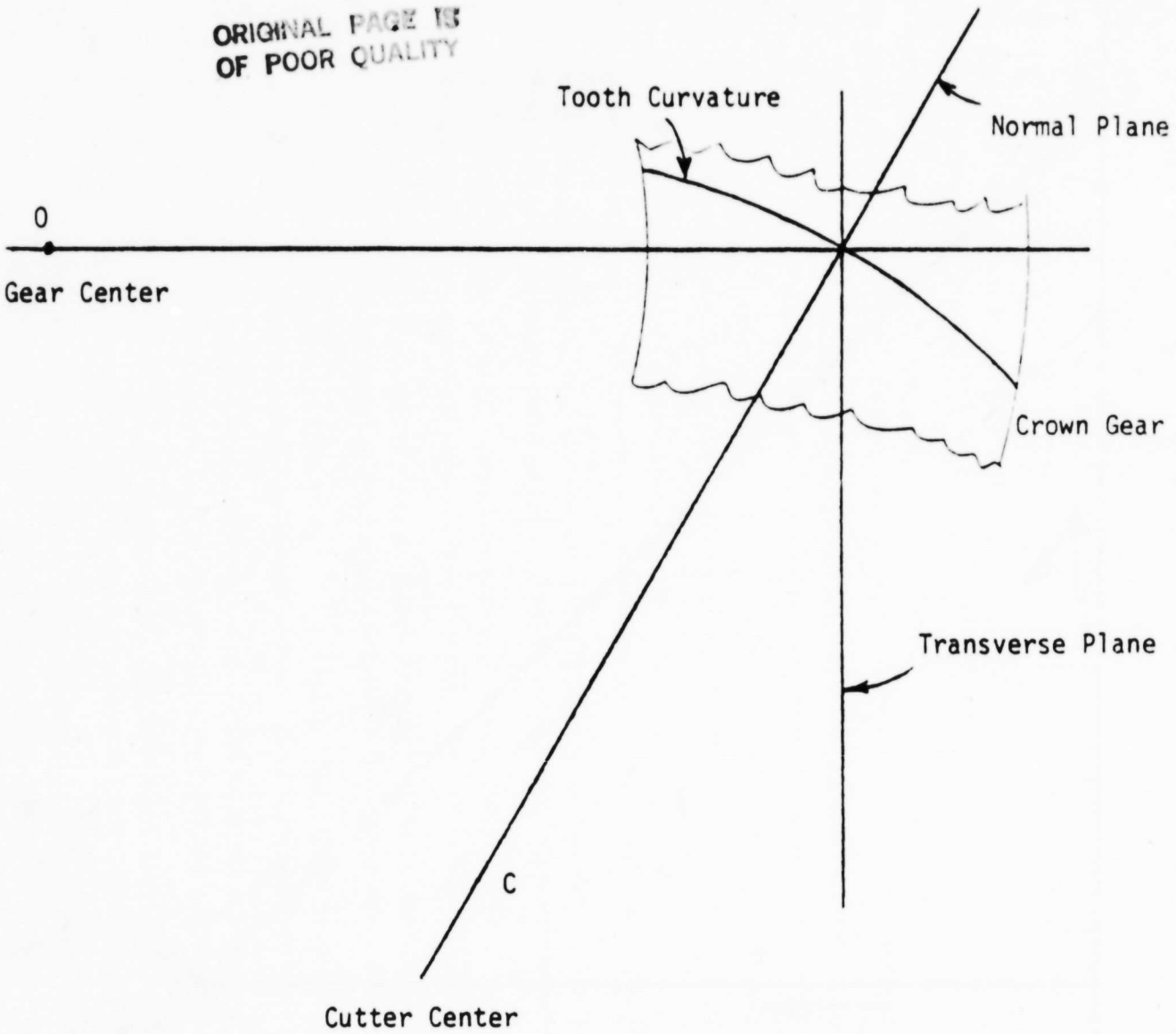

Figure 23. Gear and Cutter Centers and Edge View of Normal and Transverse Planes.

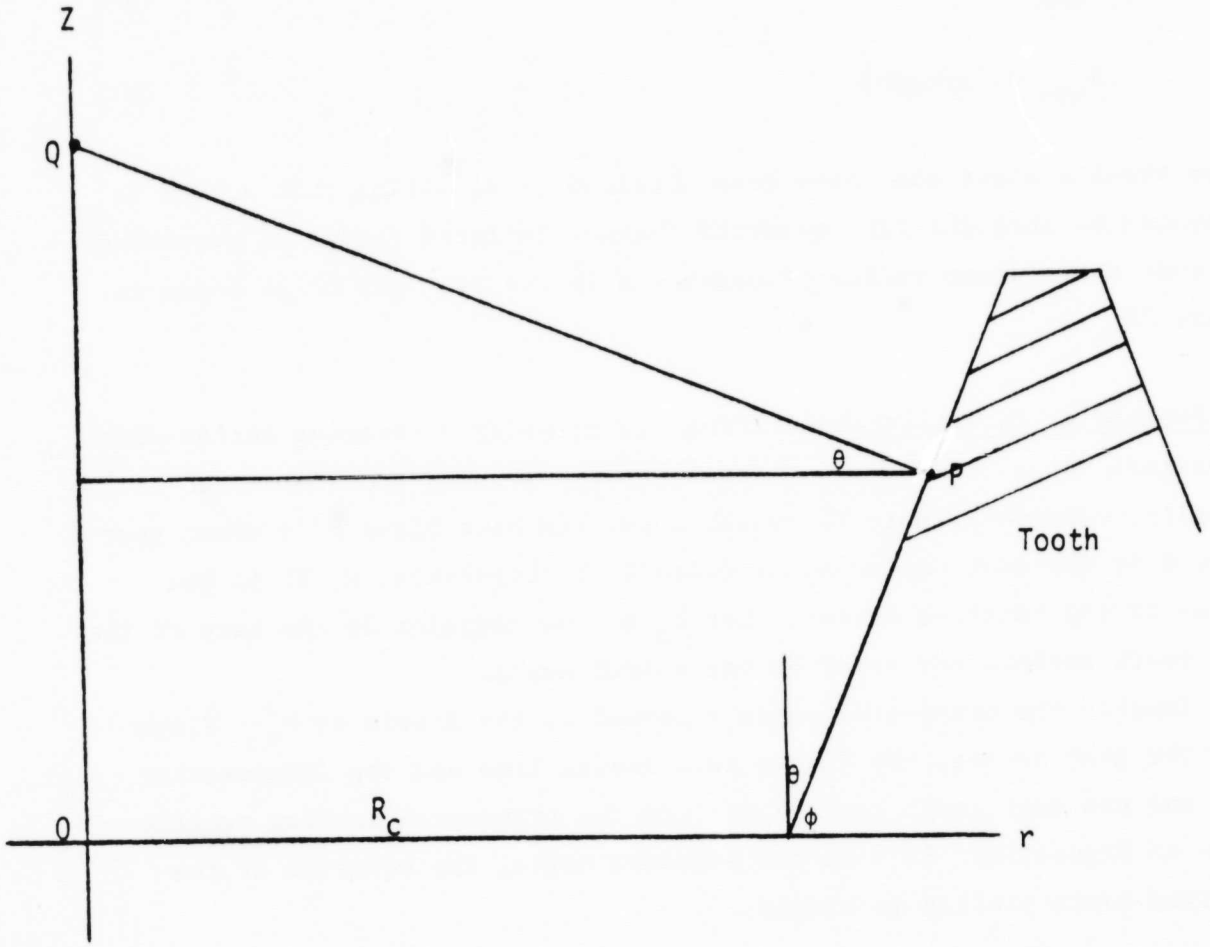

Figure 24. True View of Normal Plane Showing Crown Tooth Profile.

and

$$d^2z/dr^2 = 0 \tag{95}$$

where ϕ is the complement of θ as shown in Figure 24. Hence, Equations (79) and (80) give the maximum and minimum surface radii of curvature as:

$$R_{max} = \infty \tag{96}$$

and

$$R_{min} = |r/\cos\theta| \tag{97}$$

These results might also have been obtained by recalling that a cone is generated by straight line elements (hence, infinite radius of curvature) and that the minimum radius of curvature is the distance QP as shown in Figure 24.

3) Hyperbolic Cutter Profile. Finally, consider a rotating cutter which generates, for a crown gear, a straight line meshing profile. Specifically, consider Figure 25. which shows the base plane of a crown gear where 0 is the gear center and C (with X, Y coordinates H, V) is the center of the rotating cutter. Let P_m be the midpoint at the base of the gear tooth surface and let ψ be the spiral angle.

Imagine the transverse plane π normal to the X-axis at P_m. Since 0 is the gear center, the X-axis is a radial line and the intersection of π and the gear tooth surface defines the transverse meshing profile shown in Figure 26. If θ is the pressure angle, the equation of the inclined tooth profile is simply

$$z = y\cot\theta = ky \tag{98}$$

where z and y refer to coordinates along the Z and Y axis and k is defined as $\cot\theta$. Relative to the $\hat{X}$, $\hat{Y}$, $\hat{Z}$ axes of Figure 25. Equation (98) becomes

$$z = \hat{z} = k(\hat{y} + V) \tag{99}$$

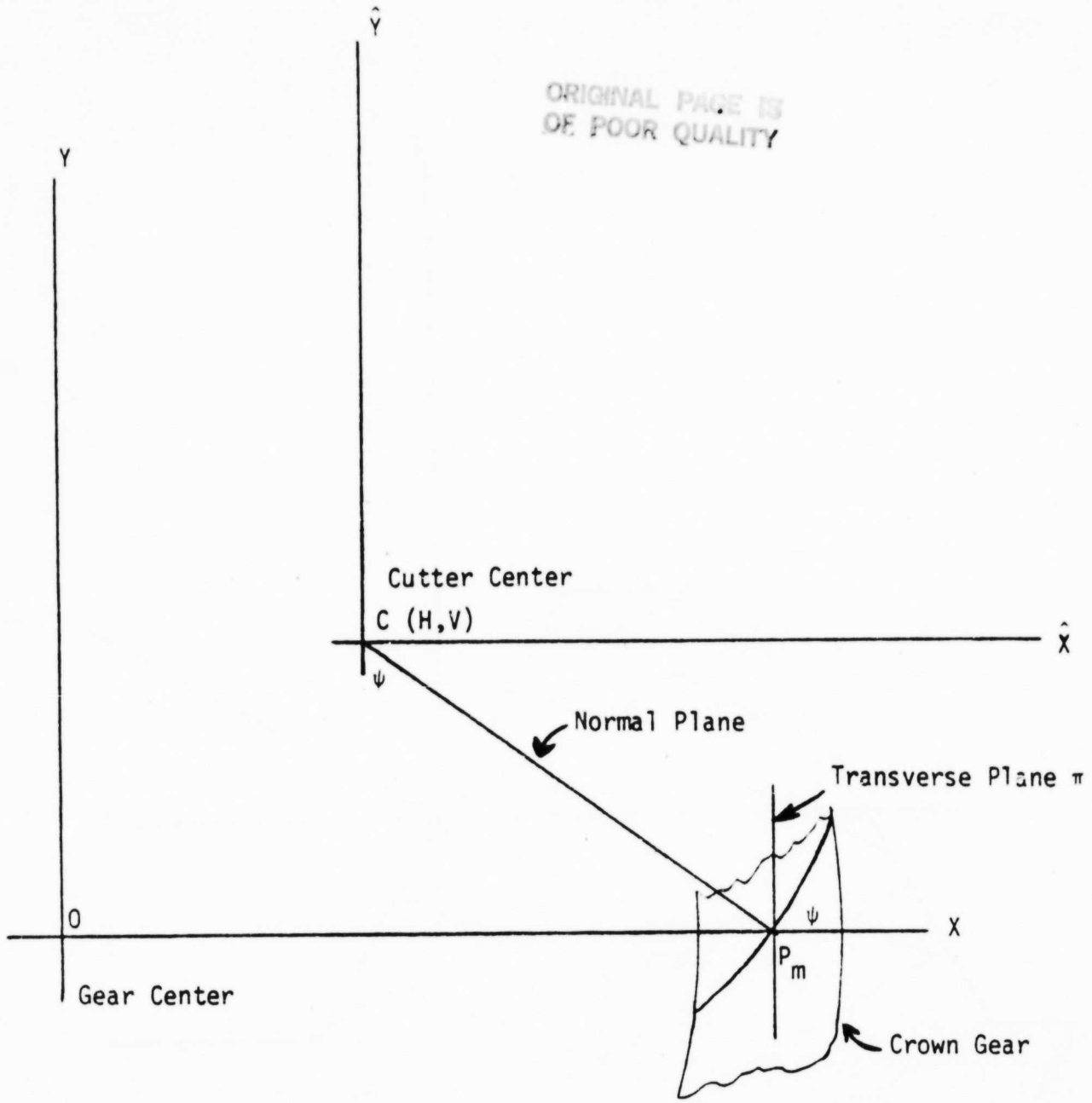

Figure 25. Crown Gear Base Plane.

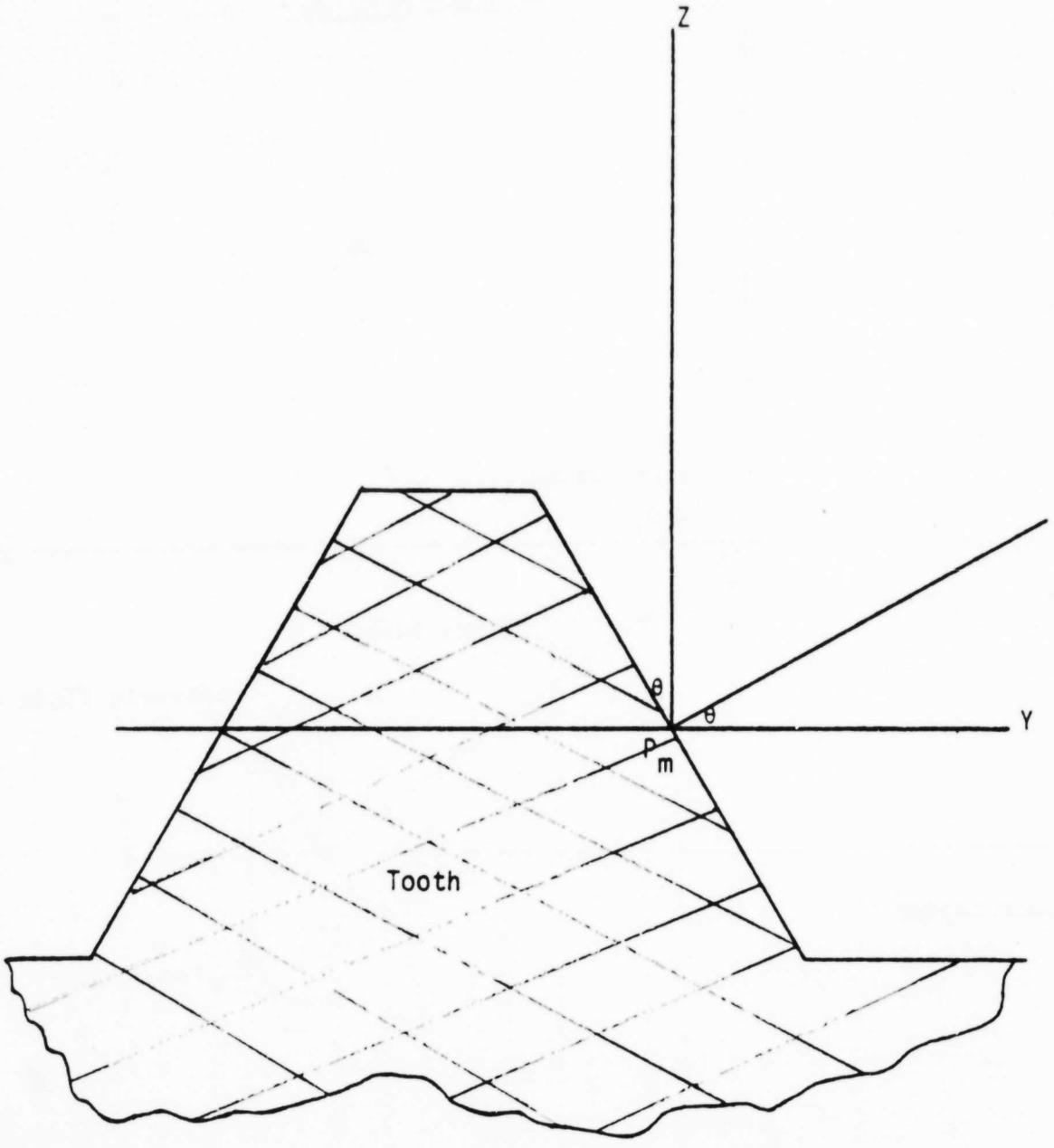

Figure 26. View of Transverse Plane π Showing Crown Tooth Profile.

In terms of $\hat{x}$, $\hat{y}$, and $\hat{z}$, the profile of the cutter radius can be expressed in general as:

$$\hat{z} = f(\hat{r}) = f([\hat{x}^2 + \hat{y}^2]^{\frac{1}{2}}) \tag{100}$$

The form of f, which defines the tooth surface of revolution, may be determined by observing that the intersection of π and the revolution surface of the cutter, must coincide with the tooth profile of Figure 26. If R_c is the distance between C and P_m, then the $\hat{X}$ coordinate of P_m is simply $R_c \sin\psi$. Hence, by letting $\hat{x} = R_c \sin\psi$ and by matching Equations (99) and (100), the following relation is obtained

$$f([R_c^2 \sin^2\psi + \hat{y}^2]^{\frac{1}{2}}) = k(\hat{y} + V) \tag{101}$$

Let $\tilde{r}$ be defined as

$$\tilde{r} = [R_c^2 \sin^2\psi + \hat{y}^2]^{\frac{1}{2}} \tag{102}$$

Then in terms of $\tilde{r}$, $\hat{y}$ becomes

$$\hat{y} = [\tilde{r}^2 - R_c^2 \sin^2\psi]^{\frac{1}{2}} \tag{103}$$

Hence, by Equation (101) f is determined as:

$$f(\tilde{r}) = k(V - [\tilde{r}^2 - R_c^2 \sin^2\psi]^{\frac{1}{2}}) \tag{104}$$

The maximum and minimum radii of curvature may now be determined directly by substitution into Equations (79) and (80), or alternatively, into Equations (75) and (76). To do this note that df/dr is

$$df/dr = -\tan\phi = -kr/[r^2 - R_c^2 \sin^2\psi]^{\frac{1}{2}} \tag{105}$$

Then r and $dr/d\phi$ become

$$r = R_c \sin\psi \tan\phi / [\tan^2\phi - k^2]^{1/2} \tag{106}$$

and

$$dr/d\phi = -k^2 R_c \sin\psi \sec^2\phi / [\tan^2\phi - k^2]^{3/2} \tag{107}$$

Hence, R_{max} and R_{min} become

$$R_{max} = |k^2 R_c \sin\psi \sec^3\phi / [\tan^2\phi - k^2]^{3/2}| \tag{108}$$

and

$$R_{min} = |R_c \sin\psi \sec\phi / [\tan^2\phi - k^2]^{1/2}| \tag{109}$$

These expressions may be written in more convenient form by expressing ϕ in terms of z. That is, by identifying z with f in Equation (104), it is readily seen that

$$r^2 = R_c^2 \sin^2\psi + [(kV - z)/k]^2 \tag{110}$$

Then, by Equation (105) $\sec^2\phi$ becomes

$$\sec^2\phi = 1 + \tan^2\phi = 1 + k^2 + [k/(kV - z)]^2 k^2 R_c^2 \sin^2\psi \tag{111}$$

Hence, R_{max} and R_{min} may be written as

$$R_{max} = \{[(kV - z)/k]^2 (1 + k^2) + k^2 R_c^2 \sin^2\psi\}^{3/2} / kR_c \sin\psi \tag{112}$$

and

$$R_{min} = \{(1 + k^2)[(kV - z)/k]^2 + k^2 R_c^2 \sin^2\psi\}^{1/2} / k \tag{113}$$

V. DISCUSSION

Perhaps the most interesting of the results are the curves of Figure 12. showing the pressure angle variation in the transverse planes for the different cutter profile shapes. In each case the variation is similar resulting in a pressure angle change of approximately 3° or 15% from heel to toe. For conical gears this change in pressure angle would be enhanced by the factor $(1/\sin\alpha)$ where α is the half-cone angle [1].

The effects of this pressure angle change on the gear kinematics, stress, and wear are unknown, but they could be significant.

The question arises as to whether it would be possible to adjust the cutter profile $f(\hat{r})$ so that the transverse plane pressure angle would be independent or r, the radial position on the gear. An examination of Equation (22) shows that f is not an explicit function of $\hat{x}$ nor $\hat{y}$. This means it is <u>not</u> possible to adjust f to make $\hat{r}/f'(\hat{r})\hat{y}$ a constant. Therefore, the pressure angle changes exibited in Figure 12. will be similar for all circular cut gears regardless of the cutter profile.

The expressions for the radii of curvature of a surface of revolution (Equations (75), (76), (77), and (78)) are applicable with circular cut crown gear surfaces of any profile. The involute profile was used as an example because of its simplicity and because of its interesting results. Also, the straight line crown profile in the transverse plane, when considered in the radial plane of the cutter, that is, the normal plane, generates a hyperboloid. Although this is a surface of revolution, it is also a "ruled surface" since it can be considered as generated by a one parameter family of lines. Equations (112) and (99) show that the maximum radii of curvature occurs when $z = kv$ or when $y = 0$, that is, at the pitch surface. Similarly, Equation (113) shows that the minimum radii of curvature occurs at the greatest elevation above the pitch surface. The implications of these results in stress, lubrication, and wear as well as the comparison with theoretical gears needs further investigation.

REFERENCES

1. Huston, R. L., and Coy, J. J., "Ideal Spiral Bevel Gears - A New Approach to Surface Geometry," Journal of Mechanical Design, Transactions ASME, Vol. 103, No. 4, 1981, pp. 127-133.

2. Litvin, F. L., and Gutman, Y., "Methods of Synthesis and Analysis for Hypoid Gear-Drives of 'Formate' and 'Helixform,' Parts 1,2, and 3," Journal of Mechanical Design, Transactions ASME, Vol. 103, No. 4, 1981, pp. 83-113.

3. Litvin, F. L., and Gutman, Y., "A Method of Local Synthesis of Gears Grounded on the Connections Between the Principal and Geodetic Curvatures of Surfaces," Journal of Mechanical Design, Transactions ASME, Vol. 103, No. 4, 1981, pp. 114-125.

4. Litvin, F. L., "Relationships Between the Curvatures of Tooth Surfaces in Three-Dimensional Gear Systems," NASA TM X-75130, 1977.

5. Krenzer, T. J., "The Effect of Cutter Radius on Spiral Bevel and Hypoid Tooth Contact Behavior," AGMA Paper No. 129.21, American Gear Manufacturers Association Semi-Annual Meeting, 1976.

6. Bonsignore, A. T., "The Effect of Cutter Diameter on Spiral Bevel Tooth Proportions," AGMA Paper No. 124.20, American Gear Manufacturers Association Semi-Annual Meeting, 1976.

7. Buckingham, E., Analytical Mechanics of Gears, Dover, 1963, pp. 338-351.

8. Baxter, M. L., Jr., "Discussion on: 'Ideal Spiral Bevel Gears - A New Approach to Surface Geometry,'" Journal of Mechanical Design, Transactions ASME, Vol. 103, No. 4, 1981, p. 133.

9. Baxter, M. L., Jr., "Basic Theory of Gear-Tooth Action and Generation," Gear Handbook, (Edited by D. W. Dudley), McGraw Hill, 1962, p. 1-16.

10. Kane, T. R., Analytical Elements of Mechanics, Vol. 2, Academic Press, New York, 1961, pp. 24,41.

11. Lipschultz, M. M., Theory and Problems of Differential Geometry, Schaums Outline Series, McGraw Hill Book Co., New York, 1969, p. 164.

APPENDIX

1. Radius of Curvature of a Logarithmic Spiral

The radius of curvature of a curve can be expressed in the form [10]

$$\rho = |d\underset{\sim}{p}/d\theta|^3 / |(d\underset{\sim}{p}/d\theta)(d^2\underset{\sim}{p}/d\theta^2)| \tag{A1}$$

where $\underset{\sim}{p}$ is the position vector to a typical point on the curve and θ is a parameter defining the locus of the points on the curve. For the plane tooth centerline in the form of the logarithmic spiral of Equation (7), $\underset{\sim}{p}$ may be expressed as

$$\underset{\sim}{p} = r\underset{\sim}{n}_r = R_m e^{\kappa\theta}\underset{\sim}{n}_e \tag{A2}$$

where $\underset{\sim}{n}_r$ is a radial unit vector. If $\underset{\sim}{n}_\theta$ is a transverse unit vector, it is easily seen that [10]:

$$d\underset{\sim}{n}_r/dr = \underset{\sim}{n}_\theta \quad \text{and} \quad d\underset{\sim}{n}_\theta/d\theta = -\underset{\sim}{n}_r \tag{A3}$$

Then, by substituting from Equation (A2) into (A1) and by using Equation (A3), ρ becomes:

$$\rho = [r^2 + (dr/d\theta)^2]^{3/2} / [2(dr/d\theta)^2 + r^2 - rd^2r/d\theta^2] \tag{A4}$$

Finally, by letting r by $R_m e^{k\theta}$ and by simplifying, ρ becomes:

$$\rho = r(1 + \kappa^2)^{1/2} \tag{A4}$$

2. Hyperboloid--A Surface of Revolution

An hyperboloid is a "ruled" surface of revolution [11]. (That is, it can be developed by straight line elements.) The equation of an hyperboloid is:

$$z^2 = r^2 - 1 \quad \text{or} \quad z = \pm(r^2 - 1)^{1/2} \tag{A5}$$

where z is the axial coordinate and r is the radial coordinate.

Equations (43) and (44) may be put into the form of Equation (A5) by the following substitution: Let

$$\xi = \hat{r}/R_c \sin\psi_m$$

$$\kappa_1 = [V + (T_0/2)]\cot\theta$$

$$\kappa_2 = [-V + (T_0/2)]\cot\theta$$

$$\zeta = R_c \sin\psi_m \cot\theta \tag{A6}$$

$$z_1 = (z - \kappa_1)/\zeta$$

$$z_2 = (z - \kappa_2)/\zeta$$

Then, by substituting the parameters defined by Equation (A6), Equations (43) and (44) take the form:

$$z_1 = -(\xi^2 - 1)^{\frac{1}{2}} \tag{A7}$$

and

$$z_2 = (\xi^2 - 1)^{\frac{1}{2}} \tag{A8}$$